

Received 24 July 2023, accepted 7 August 2023, date of publication 14 August 2023, date of current version 17 August 2023.

Digital Object Identifier 10.1109/ACCESS.2023.3304679

TOPICAL REVIEW

Embedded and Surface-Mounted Fiber Bragg Grating as a Multiparameter Sensor in Fiber-Reinforced Polymer Composite Materials: A Review

SITI MUSLIHA AISHAH MUSA^{1,2}, MOHD HAZIQ DZULKIFLI³, ASRUL IZAM AZMI^{1,2}, AND SITI AZLIDA IBRAHIM¹, (Senior Member, IEEE)

¹Faculty of Engineering, Multimedia University, Cyberjaya, Selangor 63100, Malaysia

²Faculty of Electrical Engineering, Universiti Teknologi Malaysia, Johor Bahru, Johor 81310, Malaysia

³Faculty of Mechanical Engineering, Universiti Teknologi Malaysia, Johor Bahru, Johor 81310, Malaysia

Corresponding authors: Mohd Haziq Dzulkifli (mohd.haziq@utm.my) and Siti Azlida Ibrahim (azlida@mmu.edu.my)

This work was supported in part by the Telekom Malaysia Research Fund under Project RDTC/221043, in part by the Multimedia University (MMU) Postdoctoral Researcher Fund under Grant MMUI/220125 and Grant MMUI/230002, and in part by Universiti Teknologi Malaysia under Grant Q.J130000.3851.20J06.

ABSTRACT Fiber-reinforced plastic (FRP) composites are utilized extensively in various high-end industries. Therefore, developing a proper sensing and monitoring system is crucial to monitor the production and post-production in-service structural behaviors of composite materials. This paper provides a comprehensive literature review focusing on Fiber Bragg Grating (FBG) as a multiparameter sensor in FRP composite materials. The review is mainly divided into two main themes, namely, embedded FBGs and surface-attached FBGs, followed by further sub-themes according to the application of the FBGs. Contemporary issues regarding FBGs as sensors in composite materials are also discussed. Subsequently, a comparative analysis between the embedded and surface-attached techniques from various perspectives is presented before further recommendation for the ideal embedding conditions and techniques is provided. This review is summarized with a projected view on the future of FBGs as a sensor, generally, and in composite laminates, specifically.

INDEX TERMS Fiber Bragg grating, FBG, multiparameter, sensor, composite.

I. INTRODUCTION

Fiber-reinforced composite materials, or commonly referred to as Fiber-Reinforced Plastics (FRPs) is a classification of engineering materials widely utilized in both domestic and specialized industrial applications; from water storage tanks in buildings, bicycle frames, golf clubs and rackets; all the way to hulls for fishing boats, and aircraft fuselages. As such, 50% of Boeing 737 aircraft components consist of composite materials, while Airbus increased its demand for carbon composite components by roughly 20,000 tons in 2020 [1], [2]. In view of this, it is not surprising that composite materials

are expected to reach a global market share of approximately USD 113.2 billion by 2022 [1].

The continuously rising demand for FRP composites is perhaps owed to their significantly improved properties than their predecessor constituting materials, such as a high strength-to-weight ratio, lightweight, chemically inert, low thermal expansion, and good abrasion resistance [3], [4], [5], [6]. Despite this, they are still vulnerable to defects and damage, such as broken fiber, debonding, delamination, and crack initiation, which can manifest during the fabrication stage or gradually over time while in service. Moreover, these defects are almost impossible to detect visually and can often develop into more complex ones, causing catastrophic structural integrity failures [1]. Considering the increasing industrial demand for composite materials, these defect issues

The associate editor coordinating the review of this manuscript and approving it for publication was Santosh Kumar .

necessitate the development of a reliable, highly-accurate, and portable damage detection system that allows in-situ monitoring. Based on these criteria, optical fibers are a viable candidate to be used as sensor systems in composite materials.

Basically, optical fibers are comprised of concentric-layered fiber cores and cladding of different refractive indices, enabling total internal reflection that guides the light wave propagating along the fiber [7], [8]. Typical Optical Fiber Sensor (OFS) systems often utilize single-mode fibers, with germanium oxide-doped silica as their core (approximately 8 μm in diameter) and pure-silica cladding (125 μm in diameter). Fiber optic sensing exploits the fact that external perturbations, such as fluctuation in strain, temperature, or pressure in the external vicinity of the optical fiber, impart change in phase, intensity, or wavelength of the light traveling through the fiber. These changes in light patterns and transmitted signals can be deciphered with a measuring device connected to these optical fibers and represent them as numerical values of measured external parameters, such as strain, temperature, pressure, vibration, and impact [9]. Furthermore, OFS offers numerous technical benefits, such as invulnerability to corrosion, electromagnetic and radio frequency interference, able to be easily embedded in structures, requires no constant recalibration, extensive service lifetime, and a higher safety rating due to OFS possesses no possibility to discharge high voltage or explode [7].

One type of OFS that has garnered considerable attention in the past decade is Fiber Bragg Grating (FBG) sensor. FBG is essentially a single-mode optical fiber with periodic modulation of refractive index on its core that reflects specific wavelengths of light when passing through it [9]. FBG can be configured as a competent sensing tool for varying degrees of spatial scope, from a very localized measurement (or point sensing) to broad spatial coverage with multipoint sensing (or quasi-distributed sensing). As such, it is no surprise that FBG has been widely utilized in sensing systems across numerous industrial applications over the past several decades, specifically as Structural Health Monitoring (SHM) in civil [10], [11], mechanical [12], [13], aerospace [14], [15], and electrical engineering fields [16], [17]. In this regard, FBG has also been extensively used as a sensing system in composite materials, particularly FRPs. Thus, the present in-depth review is intended to assess the significant works involving the application of FBG as a sensor in FRPs.

In the past, several research groups have published comprehensive reviews regarding FBG in composite materials. For instance, Qiu et al. [18] reviewed SHM for composites using FBG, while Lau [19] covered a more specific topic of SHM for in-composite embedded FBGs. Similarly, Kinet et al. [7] discussed the issues and challenges of SHM in composite structures using FBG. Apart from that, Kahandawa et al. [14] reviewed past research that utilized FBG for SHM in aerospace applications. Luyckx et al. [20] also elaborated on strain measurement for composite laminates using embedded FBGs and their limitations. Besides,

Takeda and Okabe [21] reviewed the feasibility of FBG as sensors in aeronautics and astronautics applications, and Tosi et al. [22] reviewed several simple and low-cost SHM systems using FBG. Leal-Junior and Marques [23] recently reviewed diaphragm-embedded optical fiber sensors, provides different insights of the fundamental aspects such as approach, materials, fabrication and sensor responses. Marques et al. [24] further discussed the possible integration of optical fiber sensing technology into aircraft monitoring systems, which include airframe monitoring, flight environment sensing, aircraft navigation, and pilot vital health monitoring. However, to the best of the authors' knowledge, no work has attempted to review the different FBG sensor deployment techniques on FRP composite laminates and discussed how these techniques might affect the sensing capabilities of the FBG or the mechanical properties of the host composites.

The rest of this paper is organized as follows: Section II presents the history and current development of FBG in various industrial applications. Section III presents the working principles of FBG as strain and temperature sensors. All the reported works are classified into two major methods of deployment, specifically embedded and surface mounted methods. Section IV provides a comprehensive review of works utilizing embedded FBG sensors in composite materials based on their main theme applications: characterization of the polymer curing process; assessment of the interlaminar mechanical and thermal properties; and damage detection and localization. Section V reports the related works of surface mounted FBG on composite laminate surfaces, which are utilized for detection and localization of damage in FRP composites and characterization of mechanical and thermal conditions. Section VII describes the important work involved with the characterization of composite FBG sensor performance. Section VIII offers recommendations for FBG embedding conditions and techniques to ensure successful measurement. Section IX discusses the practical issues and challenges of the FBG sensor implementation in FRP composite. Section X discusses the future prospects of FBG sensors that are worth further exploration.

II. HISTORY AND CURRENT DEVELOPMENT OF FBG

The pioneering work on the successful inscription of Bragg gratings on optical fibers was published by Hill et al. in 1978 [25], which was achieved by exposing the photosensitive core of a single-mode fiber to intense oppositely-propagating laser beams. Interestingly, the authors at the time proposed a possible application of these grating fiber optics as synthesized filters for lightwave communication systems. This was considered the first major milestone in establishing FBG in the sensing system. Following this, Lam and Garside investigated the factors affecting the grating parameters of FBG in 1981 [26] and were the first to report the fiber as highly responsive towards perturbation in terms of temperature change. Almost a decade later, in 1989, Meltz et al. [27] demonstrated a novel and more

practical technique of Bragg grating inscription via the side of the fiber cladding. The same research group was also the first to report using FBG as a temperature and strain sensor and predicted the possibility of FBG detecting various other parameters [28]. One can observe the continuous efforts made by the research community in the subsequent decade to properly investigate and characterize FBG, primarily focusing on improving its reliability and feasibility as a sensor [29], [30], [31].

The booming interest in FBG led to many research works utilizing optic fibers as sensors in various high-end industrial applications, including medical, oil and gas, infrastructure, aerospace, automotive, and maritime, as well as manufacturing and monitoring of advanced materials, as presented in Table 1. FRPs also became the subject of FBG sensing, mainly due to the small dimension of FBG fibers (125–250 microns) [32], allowing them to be embedded within the FRP for enhanced sensing accuracy. FBG embedment also gave birth to ‘smart composites,’ enabling in-situ SHM of numerous high-end composite structures. Until recently, conventional methods used to characterize composite structures include utilizing a strain gauge, extensometer, and thermocouple. However, multiparameter characterization could not be carried out simultaneously. As the technology progressed, strain and temperature could finally be carried out concurrently, but the machineries and equipment were enormous with limited mobility. Hence, integrating FBG sensors in FRP composite laminates allows in-situ multiparameter sensing without the constraint of space or place, which broadens the array of applications of FBG. Additionally, the proposed integration enables a more non-complex non-destructive test (NDT) and SHM of large composite-based structures, such as aircraft fuselage and wings, wind turbine blades, and offshore oil rig structures.

III. WORKING CONCEPT OF FBG

By exposing a core of single-mode optical fiber to an intense interference pattern of ultraviolet (UV) laser radiation, a series of periodically-spaced refractive index changes can be inscribed on the fiber core. The interference pattern can be attained by aligning a phase mask, which is aligned to a UV beam. Examples of UV light sources that can induce refractive index change to a photosensitive fiber include krypton fluoride laser (KrF*) (248 nm), argon fluoride laser (ArF*) (193 nm), and frequency doubled Argon ion laser (244 nm). The working principle of FBG is based on Fresnel reflection, as shown in Figure 1 [18]. The modulation of the refractive index constructively reflects light waves at a resonant wavelength (Bragg’s wavelength), in which, when a broadband light is launched into this optical fiber, a small portion of the light is reflected at Bragg’s wavelength while the remaining light is passed through.

Bragg’s wavelength for first-order grating (reflection grating) is given by [18]:

$$\lambda_B = 2n_{eff} \Lambda \quad (1)$$

TABLE 1. Details on various applications of FBG as sensors.

Field	Application/Detail	Ref.
Medical	Movement measurement for tendons and ligaments	[33]
	Joint Movement Monitoring	[34]
	Tendon force measurement	[35]
	<i>In-vivo</i> temperature measurement of the brain	[36]
	Biosensor for bone stress/deformation during ingestion pattern of living animals	[37]
	Heart sound, pulse waves, and respiration of living organisms	[38]
Wearable medical devices	Human respiratory measurement	[39]
	Hand module to measure finger joint angle	[40]
	Knee posture monitoring	[41]
Oil and gas industry	Blood pressure movement	[42]
	Hydrocarbon leak detection systems	[43]
	Oil well downhole monitoring systems	[44]
	Temperature monitoring for petroleum hydrocarbon	[45]
	Crude oil movement monitoring	[46]
	Subsea SHM	[47]
Chemistry	Multi-chemical detection and identification systems	[48,49]
	Gas flow sensors	[50]
	Temperature sensing in packed-bed non-thermal plasm reactor	[51]
	Dissolved hydrogen sensors	[52]
	Strain monitoring in concrete structures	[53]
Civil engineering	Creep monitoring in subway concrete structures	[54]
	Temperature-compensated strain measurement in arched bridges	[55]
	Crack detection and propagation monitoring in various civil applications	[56]
	Marine environment and structural monitoring	[57]
Aerospace and aeronautic	Temperature and strain sensors for harsh environments in space	[58,59]
	Aerospace smart structure monitoring	[60]
	Aircraft SHM systems	[61]

where the λ_B refers to the Bragg wavelength, n_{eff} denotes the effective mode index, and Λ is the fiber grating period. Bragg wavelength shift that occurs due to strain and temperature perturbations can be obtained from (1) [18]:

$$\begin{aligned} (\Delta\lambda_B)/\lambda_B &= (1 - p_e)\Delta\varepsilon + (\alpha + \xi)\Delta T; \\ \xi &= ((dn_{eff})/dT)/(dn_{eff}) \end{aligned} \quad (2)$$

where $\Delta\lambda_B$ is Bragg wavelength shift, α represents the coefficient of thermal expansion, ξ is the thermo-optic coefficient, and p_e is the photo-elastic coefficient of the fiber optic material, which is given by:

$$P_e = [n_{eff}^2/2] * [p_{12} - \nu(p_{11} + p_{12})] \quad (3)$$

where p_{ij} is Pockel’s coefficient of stress-optic tensor and ν is Poisson’s ratio. (2) could be expanded by substituting in (3)

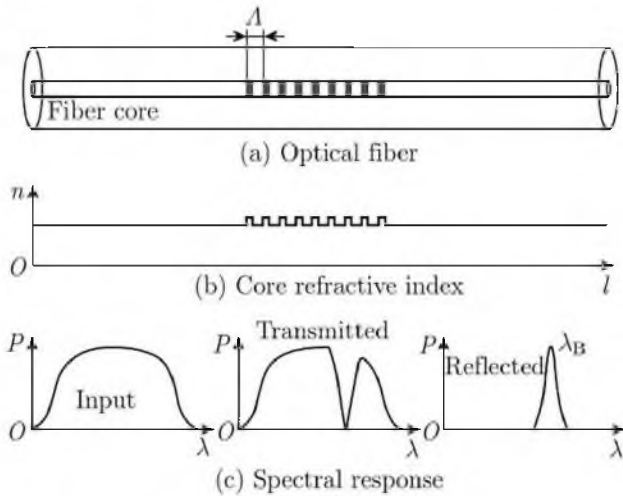


FIGURE 1. The working principle of FBG [18].

to give [18]:

$$\Delta\lambda_B/\lambda_B = [1 - (n_{eff}^2/2) * [p_{12} - \nu(p_{11} + p_{12})]]\Delta\varepsilon + [\alpha + [(dn_{eff})/dT]/n_{eff}]\Delta T \quad (4)$$

IV. FBG EMBEDDED IN COMPOSITE LAMINATES

Incorporating FBG inside composite laminates has been a widely adopted method in developing sensors, evolving the composite material into what is referred to as ‘smart composites.’ This is due to the countless benefits this method offers, which include higher sensing accuracy, reducing the risk of damage to the sensor, in-situ lifetime structure monitoring capabilities, and protection from environmental perturbation [13], [62]. However, due to its relatively complex manufacturing procedure, embedding FBG into composite laminates depends primarily on the intended application. For instance, it is more functional for the FBG to be embedded for regular in-situ SHM purposes in highly-crucial applications, such as aeronautics or aerospace. Despite this, FBG has been embedded in composite laminates with various types of fiber to measure numerous parameters – individually or simultaneously multiparameter sensing – and is intended for vast arrays of applications, as listed in Table 2.

A. CURING AND POST-CURING CHARACTERIZATION

Among the major applications of embedding FBG inside composite materials is to determine the internal temperature and strain state of the composites. In fact, several studies also compared such parameters with their external counterparts to obtain valuable information in understanding the curing mechanism of fiber-reinforced composite materials. The strong reliance on materials and mechanical properties of cured laminates to its curing regime has been well established [63], mainly contributing to the rising interest in real-time cure monitoring of FRPs. Minor variations during the curing cycle may inadvertently cause internal perturbation

in the microstructure, such as matrix cracking or delamination, or change on the external level, such as laminate warpage, that will adversely affect the properties of the FRP laminate. Furthermore, chemical crosslinking occurs during the curing process, resulting in volume shrinkage, which in turn might drive the composite laminates into an internal stress state [63]. Therefore, it is vital to learn the origins of these perturbations and control them to avoid residual strain within the composite laminates. This necessitates the incorporation of FBG as sensors inside composite materials.

Several literature studies have investigated the internal state of FRPs during curing. Previously, Guo [78] opted for a dual-FBG sensing system to simultaneously monitor strain and temperature behavior during and after the curing process of carbon composite. The temperature FBG sensor was encapsulated inside a steel capillary tube to negate the effect of thermal and/or mechanical strain, whereas the strain FBG sensor was left bare. Each of these sensors was embedded above and below the neutral plane of a 12-ply carbon/epoxy laminate stacked in an asymmetric cross-ply lay-up sequence. Since the FBGs sensors were placed perpendicular to each other, the thermal strain pattern during the curing from each sensor could be studied to predict the cured pattern of the cross-ply laminate.

Continuing their previous work [79], Kang et al. [80] embedded a hybrid FBG sensing system inside a graphite/epoxy laminate to examine its strain and temperature behavior during curing in an autoclave. Complementing this FBG sensor was an Exterior Fabry-Perot Interferometer (EFPI), which was equipped by placing two cleaved optical fiber ends inside a capillary glass tube with an air gap in between, and one end of the fiber optics was inscribed with Bragg gratings, as shown in Figure 2. In contrast to the EFPI, which was both affected by thermal and mechanical perturbations, FBG was only affected by the change in temperature since it is enclosed inside the capillary glass tube. This difference in sensing parameters enabled the simultaneous measurement with improved accuracy. However, more drastic change in strain distribution was observed, where the FBG recorded a higher transversal compressive strain compared to longitudinal strain, and the authors credited this phenomenon to the matrix reaction that largely dominated the transverse-direction properties.

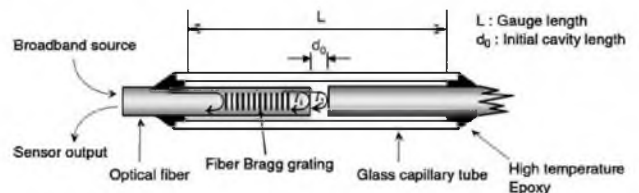


FIGURE 2. An FBG/EFPI hybrid sensor configuration [80].

Meanwhile, Yoon et al. [81] opted for a hybrid dual-FBG sensing system to characterize the curing strain and

TABLE 2. Details on selected previous literature using embedded FBG as sensors in fiber-reinforced Composites.

Details/applications	Structure	Embedding technique	Parameters	Ref.
Temperature and strain characterization in braided composites	<ul style="list-style-type: none"> - Braided composites - Glass fiber strands/vinylester resin (ER11560-F165N/Ripoxy R-802) - Curing in oven 	<ul style="list-style-type: none"> - FBG hybridized with an Exterior Fabry-Perot Interferometer (EFPI) inside a 310 μm glass tube - FBG embedded between braided glass fibers 	Curing strain, temperature, internal strain during static, and dynamic load	[64]
Interlaminar strain characterization with different embedded FBG angles and applied load angles	<ul style="list-style-type: none"> - Standard laminate specimen - E-glass woven fiber cloth/epoxy - Manufactured via hand lay-up 	<ul style="list-style-type: none"> - FBG embedded at 0°, 30°, 60°, and 90° on the 8th/9th layer 	Tensile strain	[65]
Temperature-compensated dynamic strain characterization during the fatigue test	<ul style="list-style-type: none"> - Standard laminate specimen - Carbon fiber/epoxy; [0]₂₈ - Curing in autoclave 	<ul style="list-style-type: none"> - FBG embedded during stacking at a 0° direction 	Dynamic strain, temperature due to dynamic load	[66]
FBG material and geometrical birefringence effect on composite laminates characterization	<ul style="list-style-type: none"> - Standard laminate specimen - 16-ply unidirectional carbon fiber prepregs/epoxy (M18/M55J) 	<ul style="list-style-type: none"> - Two FBGs with different birefringence - FBGs embedded on the 2nd/3rd layer 	Flexural strain, transverse load strain, temperature	[67]
SHM in aircraft wing structures	<ul style="list-style-type: none"> - Standard laminate specimen - 16-ply unidirectional and chopped-strand mat (CSM) E-glass fiber/epoxy; [CSM/0/(90/0)₃]₅ - Manufactured via vacuum bagging 	<ul style="list-style-type: none"> - No definitive information on the embedding method 	Dynamic strain, damage detection, and severity identification	[15]
Composite repair patch for aircraft composite structures	<ul style="list-style-type: none"> - Standard laminate specimen - 4- and 6-ply boron fiber/epoxy prepregs (Textron 5521); [0]₂₅, [0]₃₅ - Curing in autoclave 	<ul style="list-style-type: none"> - FBG embedded on the 1st/2nd, 2nd/3rd, and 3rd/4th layers 	Tensile strain	[68]
Transverse strain characterization using microstructured FBG	<ul style="list-style-type: none"> - Standard laminate specimen - 16-ply carbon fiber/epoxy prepregs (M18/M55J); [90₂/0₂]₂₅ 	<ul style="list-style-type: none"> - Anisotropic FBG - FBG embedded at a 0° direction on the 8th/9th layer 	Pressure, temperature, transverse strain, and axial strain	[69]

TABLE 2. (Continued.) Details on selected previous literature using embedded FBG as sensors in fiber-reinforced Composites.

	<ul style="list-style-type: none"> - Curing in autoclave 			
Vibration sensor in smart composite structures	<ul style="list-style-type: none"> - Standard laminate specimen - 12-ply unidirectional and fabric carbon fiber/epoxy prepregs; $[0_3/F_3]_S$ - Curing in autoclave 	<ul style="list-style-type: none"> - No definitive information on the embedding method 	Dynamic strain	[70]
Multiparameter characterization using Polymer-based FBG (PFBG)	<ul style="list-style-type: none"> - Standard laminate specimen - 8-ply unidirectional E-glass fiber/polyester; $[0]_8$ - Manufactured via hand lay-up 	<ul style="list-style-type: none"> - PFBG attached to the optical fiber using UV-cured adhesive - PFBG and silica FBG embedded at a 0° direction on the 1st/2nd layer 	Flexural strain and internal temperature	[71]
Simultaneous strain and temperature sensing in cryogenic conditions	<ul style="list-style-type: none"> - No definitive information on the composite specimen 	<ul style="list-style-type: none"> - Two FBGs were written on the same OF and coated with epoxy - No definitive information on the embedding method 	Temperature and thermal-induced strain	[72]
Damage detection due to low-frequency dynamic strain	<ul style="list-style-type: none"> - Standard laminate specimen - 10-ply unidirectional glass fiber/epoxy (EW200/E51); $[0]_{10}$ 	<ul style="list-style-type: none"> - Three multiplexed FBGs - FBG embedded at a 0° direction on the 2nd/3rd layer 	Dynamic strain and damage detection	[73]
Temperature sensor for composite insulators in the power sector	<ul style="list-style-type: none"> - Cylindrical composite specimen - No definitive information on the reinforcement fiber and matrix type 	<ul style="list-style-type: none"> - No definitive information on the embedding method 	Temperature	[74]
SHM for concrete structures via FBG-embedded Functionalized Carbon Structures (FCSS)	<ul style="list-style-type: none"> - Standard laminate specimen - Carbon fiber/polyvinyl alcohol (PVA) 	<ul style="list-style-type: none"> - No definitive information on the embedding method 	Flexural strain	[75]
Shape sensing of polymer core composite electrical transmission lines ACCC	<ul style="list-style-type: none"> - Cylindrical composite specimen - Carbon fiber and glass fiber/epoxy 	<ul style="list-style-type: none"> - FBG adhered to the center of the composite rod using epoxy 	Flexural strain	[76]
Swelling detection due to moisture	<ul style="list-style-type: none"> - Standard laminate specimen - 7-ply CSM glass fiber/epoxy (Airstone 780E/785H) - Manufactured via Vacuum-Assisted Resin Infusion Method (VARIM) 	<ul style="list-style-type: none"> - Two FBGs embedded at a 0° direction on the 3rd/4th layer 	Hygroscopic-induced strain and thermal-induced strain	[77]

temperature behavior of Fiber-Metal Laminates (FMLs). Bragg gratings were written on two optical fibers of different core dopants concentrations prior to being spliced together and embedded in Kevlar/Shape Memory Alloy (SMA) composites. This configuration produced a sensing system with similar sensitivity towards strain but not temperature, enabling a simultaneous strain and temperature sensing with low error margin.

Takeda et al. [82] embedded FBGs inside CFRP-stiffened composite panels, serving as a sensor system for the curing process and SHM. Figure 3 shows the FBG sensors' position beneath the interface between the panel and T-shaped stringer; one close to the longitudinal edge and the other at the center. Two FBG sensors were placed at each sensor location – one left bare and the other encapsulated inside a hollow tube to enable a strain-free environment, hence allowing simultaneous strain and temperature monitoring. The FBG exhibited an apparent lag in temperature measurement compared to extrinsically-attached thermocouples set due to the slower rate of through-thickness heat transfer. Furthermore, it was found that the position of the FBGs was not ideal, as they were located near the neutral plane of the structure.

Minakuchi [83] investigated direction-dependent post-curing shrinkage in laminate composites. In addition to the typically embedded FBGs in longitudinal and transversal in-plane directions, the authors added another FBG sensor aligned in an out-of-plane direction. With the FBG embedded through-thickness of the carbon/epoxy laminates, the FBG sensor's tail length was adjusted to consider the shear-lag effect. Consequently, it was discovered that the FBG with the longest tested tail length of 50 mm produced the most accurate curing-induced shrinkage strain measurement. It was asserted that cure shrinkage did not cause significant stress

to the transversal direction of the sensor due to it being in a uniaxial stress state. It was also suggested that using thinner and more flexible polymer-based sensors might improve the sensitivity of the sensor affected by shear-lag. In another work by the same author [84], it was noted that through-thickness temperature distribution was almost uniform for the slow-cooling cycle. A higher strain was also observed for the fast-cooling cycle due to the thermal skin-core effect. The study also reported that while long-tailed FBG is more sensitive toward strain, the difference against short-tailed FBG becomes negligible as the temperature approaches the glass-transition temperature (T_g) of the matrix.

Following this study, Hu et al. [85] utilized both short- and long-tailed FBG sensors to study the curing mechanism inside carbon/epoxy laminates. It was found that FBG with a tail length of 30 mm portrayed sufficient sensitivity to capture the strain curing process, as the difference between the strain of 30 mm and 50 mm tailed-FBG was marginal. Furthermore, FBG embedded at different laminate thicknesses exhibited no difference in strain distribution throughout the thickness, implying that epoxy resin cures uniformly in the thickness direction. The short-tailed FBG embedded in-plane and out-of-plane showed a similar strain change curve, signifying that the curing shrinkage is transversely isotropic – an identical conclusion drawn in [82] and [83].

Unlike the results by Minakuchi [83] and Hu et al. [85], Zhang et al. [86] discovered that a strain distribution exists between different layers of the composite, which might imply that laminate composite cures anisotropically in an out-of-plane direction. Prior to curing in the oven, two FBGs were embedded near the middle and surface layer of a 16-ply carbon/epoxy laminate. The strain values were obtained by calculating the wavelength shifts of both FBGs following Equation 5:

$$\Delta\lambda_{actual} = \Delta\lambda_{measured} - (\alpha + \xi)(T - T_0) \quad (5)$$

where $\Delta\lambda_{actual}$ is the shift in wavelength due to curing, $\Delta\lambda_{measured}$ refers to the shift in wavelength as measured by FBG, α and ξ are thermal expansion and thermo-optic coefficients of fiber material, respectively, and T and T_0 are the measured and initial temperatures, respectively. While the FBGs responded well to tensile loading, FBG embedded near the neutral plane of the laminate exhibited a non-linear response to bending load, which the authors assumed the non-changing length of the neutral plane under internal bending as the cause of the non-linear perturbation to the FBG.

Another work focusing on the monitoring of through-thickness-dependent parameters was reported by Chen et al. [62]. In this study, bare and stainless-steel-encapsulated FBG sensors were each embedded inside 30-ply carbon/epoxy prepregs at a 5-ply interval. Contrary to the experimental work carried out by Tsukada et al. [84], which observed no through-thickness temperature gradient inside the laminate composites, Chen et al. [62] reported approximately a 2°C temperature difference between each layer, with the peak temperature originating from the middle ply

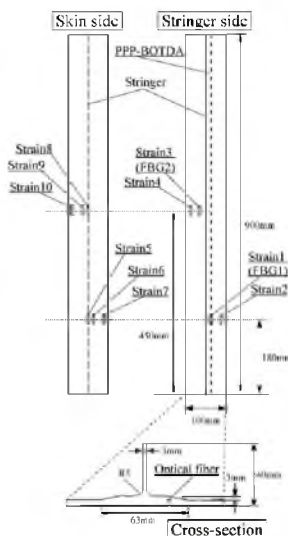


FIGURE 3. Embedment locations on a T-shaped aircraft structure [82]. Notice how the FBGs are placed both directly on the longitudinal axis and slightly offset.

and gradually decreased towards the outer layers. This phenomenon was associated with the heat released instead of chemical reactions that could not instantaneously propagate outward. While the bottom layers in contact with the manufacturing tools did allow for a more efficient heat flow – as shown by its lower temperature during the cooling stage compared to the top layer exposed to ambient air – it introduced residual strain to the composite material.

Comparing the methodologies employed by Chen et al. [62] and other works [84], [87], it could be concluded that the former was able to detect through-thickness temperature gradient in the curing stage of composite laminate due to the more effective positioning of the FBG sensors. For instance, Tsukada et al. [84] FBG was embedded directly in the out-of-plane direction compared to the in-plane direction by Chen et al. [62]. It is also highly plausible that a temperature gradient exists – or to a lesser extent, can be detected – in laminates with a high number of plies or thicknesses. Chen et al. [62] detected through-thickness temperature distribution in a 5.4 mm thick laminate, while Qi et al. [87] and Tsukada et al. [84] found none in laminates with 2.5 mm and 2.0 mm thickness, respectively.

Additionally, Rocha et al. [88] utilized small-diameter FBG to monitor the curing strain and temperature of laminated composite materials. The study inscribed two types of FBG on an 80 μm outer diameter optical fiber; one FBG is sensitive to both strain and temperature changes, while the other is only to temperature. The temperature-sensitive FBG was first enveloped inside a fused capillary silica tube. The OFS system was then embedded near the middle and bottom layers and mid-plane of 10-ply carbon/epoxy laminate composites parallel to the reinforcing fiber direction. Subsequently, the FBG-embedded laminates were manufactured via the Vacuum-Assisted Resin Infusion Method (VARIM). It was reported that wavelength shift by temperature-sensitive FBG was only due to the ambient temperature change and not from the resin reaction.

Oromiehe et al. [89] proposed a new method to compensate for temperature from strain sensing for simultaneous strain-temperature monitoring during the curing of composite laminates manufactured via Automated Fiber Placement (AFP). Two FBGs were embedded between the 2nd and 3rd ply of a 10-ply carbon/polyether ether ketone (PEEK) laminate – one longitudinally-placed, while the other was angled at 15°. A thin adhesive layer was used to securely attach the FBG to the carbon ply at a fixed 15° angle. The idea behind this proposed method is that the angled FBG will measure a slightly varied strain perturbation, and the difference in sensitivity between the axial and angled FBG could cater to the cross-sensitivity issue for simultaneous strain and temperature monitoring in composite materials. Regarding the characterization test, the authors reported that the thermal effect became less prominent as more layers piled up on the FBG sensors. This phenomenon was credited to the presence of more materials (the carbon fiber plies) between the FBG and the heat source, insinuating an evenly

distributed heat throughout the layers. However, the strain measurement exhibited a fluctuating pattern, with the trend generally increasing with increasing layers.

Matveenko et al. [90] embedded FBG with five gratings in the midpoint of a 20-ply glass/epoxy laminate and assessed the optical fiber's response toward changes in temperature and strain during the curing cycle inside an oven. The authors concluded that significant process-induced strains were detected during the manufacturing process of FRPs. In another work, the authors explored the FBG sensitivity towards inhomogeneous or non-linear strain distribution in laminate composite with unusual shapes [91]. FBGs were embedded between the 10th and 11th layer of a 20-ply glass fiber-reinforced laminate, with the composite specimens shaped into three different test coupon shapes comprising unnotched rectangular, rectangular with a sharp notch, and rectangular with a round notch, as shown in Figure 4. The specimens were then loaded with axial tensile load, and the FBG response toward change in strain was examined. Based on the results, the FBG could accurately detect the different strain gradients in the specimen under testing, as verified via a three-dimensional (3D) digital optical system, which captured data in the form of a photo.

On the other hand, Qi et al. [87] investigated the strain history of fiber-reinforced polymer composites using FBG. The authors embedded two FBGs in a transverse direction – one was left bare while the other was encapsulated in a hermetic steel tube to enable strain-free condition – in both the 1st and 5th layer of a 10-ply unidirectional carbon fiber laminate, and characterized for its curing behavior. During the FBG temperature test, the FBG curve between the 1st and 5th layers showed significant differences, which insinuated the homogenous curing of the composite. However, the bare FBGs exhibited overshoot temperature values than encapsulated FBGs due to the thermal expansion of the carbon fiber. In fact, it was reported that during the curing cycle, the embedded FBGs could register thermal strains from exothermal chemical reactions, compressive strains due to

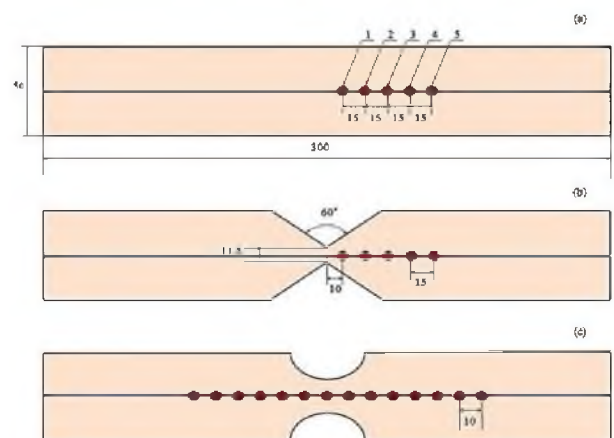


FIGURE 4. Different-shaped laminate composite specimens tested in [91].

curing shrinkage, and thermal strains due to a mismatch of the thermal expansion coefficient for carbon fiber and epoxy resin.

Boateng et al. [92] investigated the suitability of different capillary tubes in thermal strain isolation to embed FBG in composite material curing behavior monitoring. Three different types of strain-isolation casings – one made from glass while the other two from steel of different diameters – were used to envelop a standard FBG, with both ends of the casing fixed onto the FBG using an epoxy sealant. The encased FBGs were embedded in axial and transversal directions inside unidirectional carbon fiber reinforced composites. Comparatively, the glass capillary casing showed almost zero sensitivity towards the varying heat rate compared to the steel capillary due to the difference in the thermal expansion coefficient between the two strain-isolation casings. Of the two embedding directions, the FBG in the perpendicular direction detected a higher amount of strain relative to that in the parallel direction. The authors also claimed that it was difficult to accurately distinguish between strains due to the curing shrinkage and strain due to the fiber expansion from the FBG strain curve.

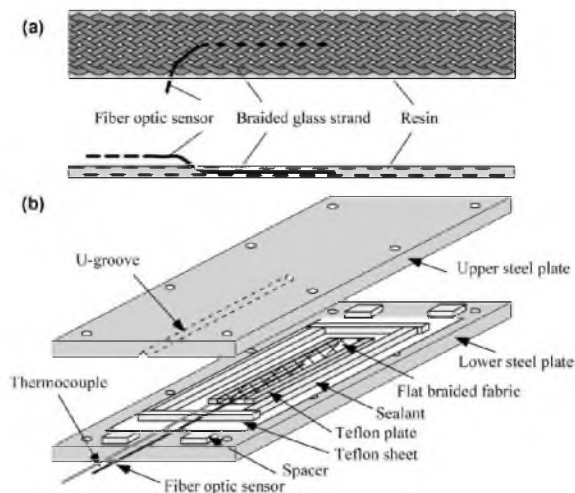


FIGURE 5. a) Configuration of OFS embedment into braided composites; (b) Experimental setup for the in-situ monitoring of composite curing inside a customized mold [64].

B. INTERLAMINAR MECHANICAL AND THERMAL CHARACTERIZATION

Apart from monitoring curing and post-curing conditions, FBGs are frequently embedded in composite laminates to obtain their hosts' mechanical and thermal characteristics. Unlike the internal source of strain and temperature change related to the curing and post-curing monitoring in Sub-Section IV-A, this section discusses FBG as an embedded sensor for external sources of strain and temperature perturbations. It is vital to precisely characterize the strain and thermal properties of the laminates to avoid any catastrophic in-service failure of the laminate. This is achievable by embedding FBG at strategic locations to allow for more

accurate sensing, as FBG reacts directly to its surrounding perturbation [13]. Apart from that, proving the feasibility of FBG as an interlaminar sensor for composite laminates allows for more diverse subsequent applications, specifically SHM, which involves periodic interlaminar strain and thermal monitoring. This is also perhaps the main reason for the rising interest in utilizing FBG as sensors in smart composite structures.

Previously, Frazao et al. [93] explored an alternative configuration to correctly discriminate between strain and temperature in simultaneous FBG sensing by adopting the different strain responses of FBG in numerous composite laminate layers. Mathematically, the expression can be presented as:

$$\begin{bmatrix} \Delta\lambda_{\text{FBG1}} \\ \Delta\lambda_{\text{FBG2}} \end{bmatrix} = \begin{bmatrix} b_1 & 0 \\ b_2 & 0 \end{bmatrix} + \begin{bmatrix} K_{T1} & K_{\varepsilon 1} \\ K_{T2} & K_{\varepsilon 2} \end{bmatrix} \begin{bmatrix} \Delta T \\ \Delta \varepsilon \end{bmatrix} + \begin{bmatrix} a_1 & 0 \\ a_2 & 0 \end{bmatrix} \begin{bmatrix} \Delta T^2 \\ \Delta \varepsilon^2 \end{bmatrix} \quad (6)$$

where K_T and K_ε represent the temperature and strain coefficients, respectively, ΔT and $\Delta \varepsilon$ denote the change in temperature and strain, respectively, and a and b are empirical constants. The authors embedded an FBG between two and four layers of carbon fiber prepregs prior to curing in an autoclave. As expected, strain characterization at a constant temperature exhibited linear but distinguishable differences between the two FBGs. Nevertheless, temperature characterization at constant strain showed a non-linear response, with a marginal difference between the two curves from the two FBGs due to the different wavelength responses to temperature perturbation.

Kosaka et al. [64] tested the feasibility of using FBG as a strain and temperature sensor in braided composites. FBG was coupled with EFPI and embedded inside glass fiber braids along with a thermocouple (Figure 5(a)) prior to being impregnated with epoxy and cured inside a customized mold (Figure 5(b)). The braided glass fiber-reinforced plastic (GFRP) test specimens were then loaded with tensile and dynamic loads. During the mechanical testing, the FBG reading exhibited a peculiar anomaly in which after the strain reading was measured correctly up until 0.8% strain – as verified via the externally attached strain gauge – the FBG output reading drastically ‘hopped’ discontinuously. The discrepancy between the strain gauge and FBG feedback rose as the experiment progressed. The FBG spectra also depicted spectral distortion, beginning with a spectral broadening at lower strain values and developing into peak splitting as the strain increased. Further investigation revealed that this phenomenon was due to the damage initiation or crack nucleation near the sensor gratings, which caused non-uniform strain distribution along the sensor grating. Following this, a similar observation was observed during the dynamic mechanical test in which, after reaching approximately 15,000 load cycles, the emergence of smaller peaks can be detected for FBG spectra. Close-up photography revealed the presence of numerous matrix cracks in the vicinity of the sensor, which was assumed

as the cause for the spectral distortion of FBG spectra in the said fatigue test.

Alternatively, Mulle et al. [94] explored the feasibility of FBG as sensors to detect strain change of quasi-static indentation and low-velocity impact load in thermoplastic composites. The study staked eight layers of unidirectional glass fibers in a cross-ply direction for the hot press manufacturing method with polypropylene (PP)/rubber copolymers as the matrix. FBGs were embedded inside the surface layer of the composite, near the 0/90-layer interface. The results observed a significant signal loss in the FBG sensor due to indentation (between 4 and 6 mm). The finding was associated with the altered light path due to the severe micro-bending experienced by the optical fiber. Strain change between the top and bottom plane of the specimens, as well as the loading-unloading strain path, were asymmetrical due to load-induced damage. Moreover, the study deduced that FBGs were more sensitive toward transversal tension and longitudinal compressive loading, and the FBGs suffered no apparent damage under low-velocity impact loading that could impair their sensing capabilities. Interestingly, wavelength hopping was observed during a low-velocity impact loading due to the FBG sensing non-uniform strain distribution, which in turn caused spectrum division.

Furthermore, Keulen et al. [2] utilized multiplexed FBG and Etched Fiber Sensors (EFSs) as flow and strain sensors to develop composite structures via the Resin Transfer Mold (RTM) process. The authors fabricated two different specimens. The first consisted of a multiplexed OFS embedded in the surface layers of an 18-ply plain-weaved glass/epoxy composite laminate, while the other sample was a 6-ply glass/epoxy semi-circular composite structure, with the OFS embedded between the 4th and 5th layer. The EFS was intended to detect resin flow during the RTM process, while the FBG was used to detect strain in the manufactured composite. Accordingly, the FBG was able to detect strain in both laminate and semi-circular composites with an average sensitivity of $1.288 \text{ pm}/\mu\epsilon$. The difference in values compared to the typical strain sensitivity of FBG was credited to several manufacturing, processing, and material errors. The authors also reported an interesting observation, where the multiplexing arrangement between the FBG and EFS resulted in no change in the power output when the mold was saturated with resin.

Meanwhile, Basu and Ghorai [65] determined the effect of FBG embedding angle and load angle on its strain-sensing capabilities inside composite materials. An FBG was embedded at different angles between the 8th and 9th plies of a 16-ply glass/epoxy laminate composite for each specimen prior to being loaded with tensile load, and its effect on the strain sensitivity of the FBG sensor was precisely assessed. The schematic representation of the embedding angle of FBG between the lamina and inside test specimen is illustrated in Figures 6(a) and 6(b), respectively. It was revealed that as the angle increases (i.e., the sensor angle becomes perpendicular to the direction of applied load), variation in

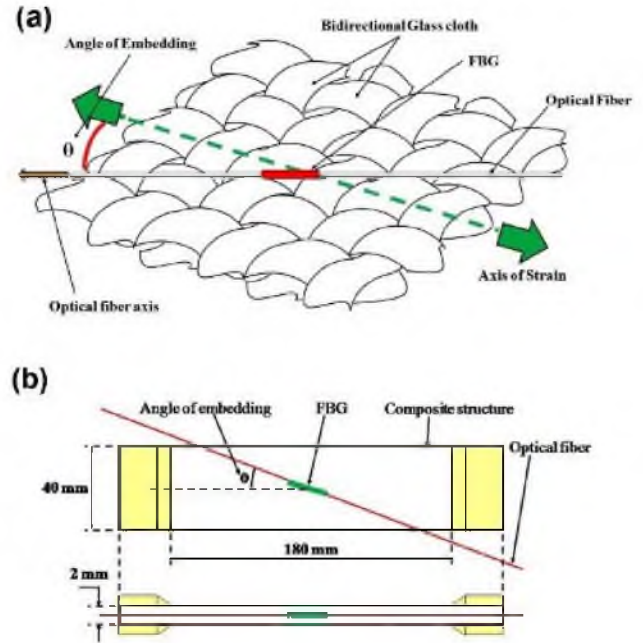


FIGURE 6. Schematic representation of the angled FBG embedment (a) inside the woven glass fiber fabric layer, and (b) inside the tensile test specimen [65].

the reflected optical power decreases, with both experimental and theoretical values exhibiting similar trends within an acceptable margin of error. For the case of different loading angles, almost identical findings were observed, in which the detected strain and variation in reflected optical power reduced with an increase in loading angle.

Recently, Papantoniou et al. [68] simulated the patching or repair of aircraft composite structures by manufacturing a unidirectional boron/epoxy composite with FBGs embedded just below the last layer of the composite laminate. Another batch of specimens was manufactured to investigate the effect of FBG embedment on the microstructure and properties of its host composite material. Several FBGs were placed between the manufactured boron/epoxy plies, parallel in the direction of the reinforcing fiber. It was revealed that the presence of FBG in the composite laminate adversely affected its tensile properties to a certain degree – a reduction of approximately 300 MPa was observed. This decrease was owed to the manufacturing errors manifested with FBG implanted in the laminates, such as local debonding and delamination. Further exacerbating this finding was a further drop of 100 MPa when the FBG was offset from the specimen's neutral axis, which was presumed to be attributed to the additional bending effect exerted by the optical fiber. Another factor that could contribute to the decline of mechanical properties was the disparity in the diameter size between the reinforcing and the optical fiber. Since optical fibers, such as FBG, often possess significantly larger diameters than individual reinforcing fibers, they tend to act as defects or stress concentrators within the reinforcing microstructure of composite laminates.

On the contrary, Kuang et al. [95] demonstrated the sensing capabilities of FBG in FMLs and FRPs. FBGs were embedded approximately on the middle layer of an 8-ply glass/epoxy and carbon/epoxy laminate. Conversely, the FMLs comprised of 7-ply glass/PP alternated with aluminum sheets with the FBG embedded near the surface plies. The stacking sequence between the specimens was varied, in which quasi-isotropic, unidirectional, angle-ply, and cross-ply configurations were employed and tested. Comparing the spectra pattern between pre- and post-curing, it was revealed that unidirectional FRPs and FMLs exhibited no spectrum distortion. In contrast, the quasi-isotropic showed a slight distortion, while the angle-ply FRPs showed peak-splitting. The occurrence of peak-splitting was due to the non-uniform strain distribution exerted on the FBG sensor, which could be introduced by the adjacent 45° angle-ply-stacking sequence. For cross-ply FMLs and FRPs, it was discovered that the FBG sensor was ‘nestled’ inside the adjacent longitudinally-parallel glass-fiber layers, which consequently was suspected of causing the radial compressive strain exerted on the sensor grating to reduce.

In addition, Mohanta et al. [77] used FBG to measure swelling in composite materials due to water immersion. The FBG and thermocouple were embedded between the 3rd and 4th layer of a 7-ply glass/epoxy, and the laminate specimens were manufactured through VARIM. The test specimens were then immersed in corrosive-produced water at room temperature and standard atmospheric conditions for a set period, while the readings from the FBG were recorded at a certain period to assess the strain state in the GFRP specimens due to water-absorption swelling. The study reported a strong correlation between the deterioration in mechanical properties and the increase in specimen weight due to water absorption with the hygroscopic strain, defined as strain exerted within the composite specimen due to swelling and changes in the fiber-matrix interface. The strains can be mathematically represented as:

$$\begin{aligned} \varepsilon_{meas} &= c\Delta M(t) - X(a)^m; \\ a &= (P_o - P_t)/P_o \end{aligned} \quad (7)$$

where c refers to the isotropic linear Coefficient of Moisture Expansion (CME) of polymer, ΔM represents the weight gained by the specimen at time t , X and m denote empirical constants, and P_o and P_t signify the material properties at the initial time and at time t , respectively.

C. DAMAGE DETECTION AND LOCALIZATION

The previous sub-sections discussed the techniques used to embed FBG in FRP laminates as sensors to monitor its curing and post-curing internal state and to characterize its host composites’ mechanical and thermal properties. Hence, this sub-section elucidates the function of FBG specifically to detect internal microstructural damages in composite laminates, such as debonding, delamination, fiber breakage, and matrix cracks, known as Barely Visible Damage (BVD).

While some of these damages have been discussed in Sub-Section IV-B, they were mainly due to external tensile or compressive load. Oppositely, this sub-section focuses on the artificially-caused damage to emulate real-life application damages. This section also elaborates on the utilization of FBG in detecting external impact events on composite structures and triangulating or localizing the impact’s source location. One of the most common types of loads experienced by high-end in-service composite structures, such as commercial aircraft and wind turbine blades, is low-velocity impact. While most impact damages can be detected by the naked eye (such as dent, breakage, or puncture on structures), some are not. These damages are called Barely Visible Impact Damage (BVID), which are impact-induced BVDs and can dramatically increase the possibility of structural failure. In this case, FBG is an indispensable approach to assess the internal state of the composite material, specifically in detecting BVIDs. Not only is it crucial to be alerted to the occurrence of impact events, but the information on the impact location should also be known so that proper maintenance and repair can be carried out on the affected area. FBG also plays a role in impact source triangulation.

Oromiehe et al. [12] explored the feasibility of using a dual-FBG sensor system for damage detection in AFP-manufactured laminates. A single FBG sensor was longitudinally-embedded between the 2nd and 3rd layer of unidirectional glass fiber, followed by placing an artificial overlap defect on top of the FBG sensor to emulate the delamination defect and crack growth. The study evaluated the wavelength shift curve of both damaged and defect-free specimens and proved that the damaged laminate spectrum exhibited a less prominent peak than the defect-free specimen when the placement head passed through the FBG sensor area. The authors further elucidated that the finding was due to the presence of artificial unstacked overlap on top of the FBG sensor, acting as a heat inhibitor that hampered a proper transfer of heat from the placement head to the sensor.

Okabe and Yashiro [96] also investigated the capability of FBG as a damage-detection sensor in composite laminate structures. An 8-ply carbon/epoxy composite laminate was manufactured containing an FBG sensor embedded between the 3rd and 4th layer and positioned approximately 1.5 mm offset from a 5-mm diameter hole drilled at the center of the specimen. Tensile and cyclic loads were then applied to the manufactured specimens. The broadening FBG spectrum was observed post-embedding, which was associated with the birefringence effect of residual thermal strain due to the curing of the laminates. During tensile load, the FBG spectrum changes according to the damage state near the hole, especially upon splitting and delamination, in which the spectrum showed peak splitting and the emergence of numerous minor peaks. However, during the dynamic load test, FBG spectra showed almost no change in pattern, although apparent damage had already occurred on the specimens, which were confirmed via soft X-ray photography, as portrayed in Figure 7. Upon closer inspection, it was discovered that this

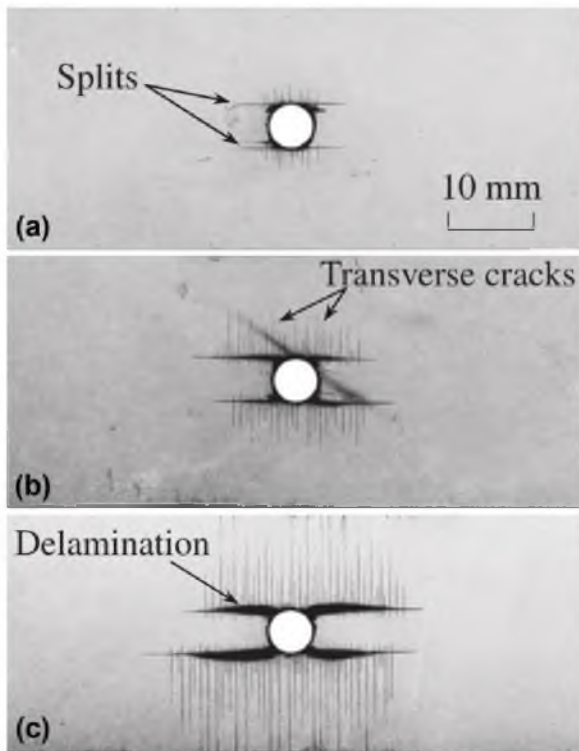


FIGURE 7. a) Configuration of OFS embedment into braided composites; (b) Experimental setup for the in-situ monitoring of composite curing inside a customized mold [96].

phenomenon was due to the debonding between the optical fiber and the composite, which did not occur during the static load test. These findings were almost similar to their previous study [97], where notches were made on each transverse side of the specimens rather than drilling a hole at the center of the specimen. In addition, the authors found that since the split defect caused stress concentration at its tips, the FBG tends to react strongly if the damage occurs near the vicinity of the sensor gratings, which indirectly implies the importance of proper sensor orientation and placement inside composite laminate structures.

In one study, Prusty and Raju [98] proposed a damage detection method in offshore composite structures by utilizing Acoustic Emission (AE) and FBG as sensors. Top-hat-shaped composite stiffened panels (Figure 8) were manufactured using an 8-ply glass/vinylester combination and cured under room temperature conditions prior to being loaded with tensile load until fracture. One phase of the study involved embedding the FBG fiber inside the curved section of the crown-web bend region. The findings revealed that FBG could accurately detect damage occurrence and its progression, size, and location inside the composite structure through a sudden fluctuation of strain distribution or a sudden spike in strain gradient. Nonetheless, the authors argued that the current methodology was limited to localized damage detection, restricting its wider application.

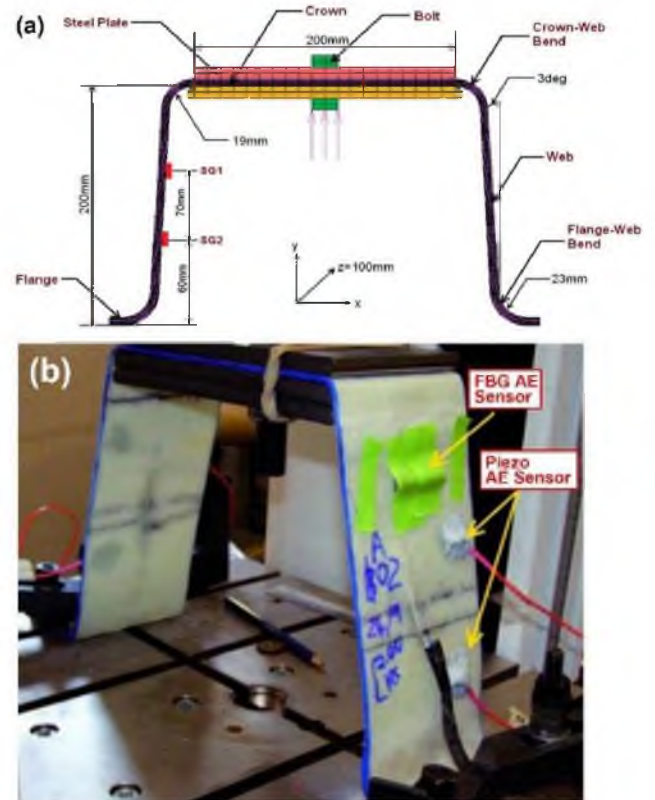


FIGURE 8. a) Configuration of OFS embedment into braided composites; (b) Experimental setup for the in-situ monitoring of composite curing inside a customized mold [98].

Freire et al. [99] explored the potential of FBG as a strain sensor for industrial steel piping applications reinforced with composite laminates. In this study, steel pipe specimens suffering from metal loss area were repaired via patching with 12-ply carbon/epoxy laminates. Two FBG sensors were each embedded between the layers of the composite laminate patching (one at 0° and the other at 90° circumferentially away from the defect region). Another three FBGs were directly attached to the defective surface of the steel pipe. The pipe was then pressurized under several conditions until it burst. Based on the results, a higher pressure reading was detected closer to the defect area, specifically the FBG between the layers closer to the base of the metal loss defect. Similar findings were also observed for strain distribution through-thickness of the repair patch, where the FBG recorded higher strains on the inner layers.

Working with 3D-braided composite structures, Li et al. [100] utilized FBG as a strain sensor for SHM purposes on the said structure. The FBG sensor was embedded during the 3D weaving process comprising a carbon/epoxy combination with the braiding angle and sensor spacing and manufactured via the RTM process. At a lower braiding angle, it was revealed that the FBG wavelength peak change exhibited a non-linear relation with its applied strain, as measured and verified via a strain gauge. It was believed that additional bending exerted on the sensor exists at a

lower angle, and this effect gradually disappears as the braiding angle increases. The same author [101] investigated 3D six-directional braided composites with embedded FBG for damage detection. Similarly, the specimens were manufactured via RTM consisting of carbon/epoxy composites, and several types of mechanical damages were imposed on the specimens post-curing, such as impact damage, internal cracks, holes, and linear scratches. Distinguishable fluctuations of the wavelength peaks were observed for composites with existing damages compared to that of pristine ones.

Moreover, Rajabzadeh et al. [102] employed FBG to detect the BVD of transverse cracks in composite laminates. The FBG was embedded between the 4th and 5th layer of a 24-ply carbon/epoxy laminate and between the 2nd and 3rd layer of a 10-ply glass/epoxy laminate. The specimens were then subjected to tensile load until the crack formation was visibly detected via camera. It was found that FBG in CFRP specimens exhibited wavelength anomaly in peak broadening, owing to the presence of residual strain. This anomaly was thought to be due to the manufacturing process, as GFRP specimens fabricated without being subjected to high transverse pressures suffered marginal to no residual strain. Hence, the FBG spectra were less affected by the birefringence effect than its carbon fiber-based counterpart. Upon the nucleation of the first crack, the FBG spectrum visibly changed shape, with a particularly interesting observation being the emergence of new harmonics on the side-lobe spectra. Therefore, the authors inferred that the FBG reflection spectrum side-lobes were highly-reactive toward the change in strain distribution along the sensor grating. Also worth being pointed out was that since the study was limited to detecting the formation of up to two cracks only, it is highly plausible that the formation of cracks more than this could be more challenging to localize.

V. FBG MOUNTED ON COMPOSITE LAMINATES SURFACE

As opposed to being permanently embedded inside its host composite materials, another feasible method to employ FBG as a sensing system in fiber-reinforced composite laminates is by physically mounting the OFS on the surface of the composites. Epoxy is the most common adhesive used to attach FBG to the composite surface, which is usually the preferred resin for the composite system, although it is not unusual to use other types of adhesives. Apart from the simplicity of employing this method, attaching the OFS on the external surface of the FRP laminates also offers numerous other benefits compared to embedding them inside the composites, such as non-complex maintenance and the ability for visual inspection of the sensor [103]. Attaching FBG on the external surface is also done to suit specific fabrication or manufacturing limits that are unsuitable for embedding the FBG, such as to perform SHM on enormous composite structures, for example, aircraft cockpit or fuselage, or even composite bridge. As shown in Table 3, externally-mounted FBG sensors system has also been utilized in various applications, measuring multiple parameters in different composite

types. As such, the following in-depth literature review is categorized by their theme applications, namely for damage detection and impact source sensor, as well as for mechanical and temperature characterization. The first sub-section reviewed numerous works in the past that covered damage detection, severity identification, and impact source triangulation or localization method using externally-mounted FBGs. The final sub-section encompasses past literature studies that utilized FBG to obtain the mechanical and thermal properties of the tested FRPs.

A. DETECTION, SEVERITY, AND LOCALIZATION SENSOR

It is unsurprising that among the typical applications that require the FBG to be externally attached to the surface of composite laminate structures are those related to damage detection and its severity. The damage source triangulation and localization also use FBG as part of the sensor system. Since some of the composite structures are large by design, such as aircraft cockpits, wings, and fuselage, as well as wind turbine blades, it is more feasible to attach the sensor system on the external surface of the structures for in-situ monitoring. Past works focused on this theme include that by Wu et al. [112], who explored the damage detection aspects of FBG sensors in composite materials by integrating them with Piezoelectric transducer (PZT). Three FBGs and two PZTs were fabricated on a composite patch to form a damage detection zone prior to being mounted on composite test specimens. The center of the zone of the specimens were then impacted to introduce damage, and subsequently to observe the impact and damage-sensing capabilities of the smart sensing system established. The first test phase involved mounting a stick-on patch across the path between FBG and PZT, which revealed slightly different spectra than the unperturbed sensor system. This was due to the high composite stiffness of the panel, which reduced the effect of flexural wave propagation. The second phase involved the controlled impact damage via hammering a rod on the specimen to introduce damages, such as delamination, debonding, and cracks. Pitch-catch test of the damaged specimen revealed a significant alteration in the spectra's phase and amplitude due to the debonding damage.

Shin et al. [107] deployed distributed FBG to monitor the impact load on wind turbine blades. Nine pairs of longitudinal and transversal FBG sensors were positioned externally on various locations of a retired 22-m long 660 kW wind turbine blade surface. The impact events were simulated using a hammer on a known and coordinated location on the blade surface. However, the authors claimed that it was impossible to regulate the applied impact due to the difference in the blade's structural response to the force. Furthermore, the focus of the study was more on assessing the capability of FBG sensors in detecting impacts rather than detecting their severity. Regardless of the fiber orientation or impact location, there was always an FBG sensor that successfully detected an impact event, which could be separated from the background noise. For cross-region impact events, it was also observed that FBGs positioned longitudinally towards

TABLE 3. Details on selected previous literature studies using FBG as a sensor on the external surface of fiber-reinforced composites.

Details/applications	Structure	Surface-mounting technique	Parameters	Ref.
Strain and temperature characterization in 3D-braided composites	<ul style="list-style-type: none"> - 3D-braided composites - Carbon fiber strands/epoxy - Manufactured via RMT 	<ul style="list-style-type: none"> - FBG hybridized with EFPI and encapsulated in 300 μm - FBG/EFPI mounted on the surface of the specimen with glue 	Tensile strain and temperature	[104]
Damage and degradation detection in bolted-joint composites	<ul style="list-style-type: none"> - Bolted-joint composite structure - Glass fiber/epoxy 	<ul style="list-style-type: none"> - Two FBGs were placed through-thickness of the composite plate - FBGs mounted using adhesive Scotchweld DP100/DP270 	Strain (creep)	[105]
Pressure sensing	<ul style="list-style-type: none"> - Hollow cylindrical shell - Carbon fiber ribbon/epoxy (UP-01/EZ-LAM) - Manufactured via filament winding 	<ul style="list-style-type: none"> - An FBG pre-strained and fixed through cylinder shell end-caps holes using epoxy 	Pressure	[106]
Impact detection in wind turbine blades via distributed FBG	<ul style="list-style-type: none"> - Wind turbine blade structure - No definitive information on the composite makes and manufacturing 	<ul style="list-style-type: none"> - 18 pairs of FBGs attached to specimen surface at 0° and 90° direction; 6 pairs divided into three regions each 	Impact damage detection, severity identification, and localization	[107]
Damage detection in aircraft structures due to dynamic load	<ul style="list-style-type: none"> - Aircraft panel (skin, stringer, and frame) - Carbon fiber/epoxy prepregs (Sigrafil CE 1007/E022); [0/90/45/0/-45/90]_s, [0/90/\pm45]_{2s}, [0/90/\pm45]_s 	<ul style="list-style-type: none"> - Three FBGs mounted on the frame, one on the skin using adhesive 	dynamic strain, damage detection	[108]
Damage localization in aircraft structure due to low-velocity impact	<ul style="list-style-type: none"> - Aircraft wing structure - No definitive information on the composite makes and manufacturing 	<ul style="list-style-type: none"> - Indefinite information on the surface-mounting method 	Impact damage localization	[109]
Matrix crack detection sensor in composite laminates	<ul style="list-style-type: none"> - Standard laminate specimen - E-glass unidirectional fiber/epoxy (EKU1150(0)/SWANCOR 2711-A BT; [0_n/\pm90_m/0_n], m and n are integers - Manufactured via VARIM, oven-cured 	<ul style="list-style-type: none"> - An FBG was attached to the center of the test specimen using glue 	Tensile strain	[110]
Vibration monitoring in composite automotive roof structures	<ul style="list-style-type: none"> - No definitive information on the composite makes and manufacturing 	<ul style="list-style-type: none"> - 8 FBGs were placed at pre-determined locations via numerical optimization 	Impact strain and displacement	[111]
Brittle fracture monitoring in composite insulators	<ul style="list-style-type: none"> - Transmission line composite insulator structures - No definitive information on the composite makes and manufacturing 	<ul style="list-style-type: none"> - Five FBGs were written on a single OF - Each OF mounted axially separated 120° from each other about the centroid of the structure 	Tensile strain and damage detection	[16]

the impact location origin exhibited more sensitive detection. Impact locations can also be predicted by computing the wave speed of the impact signal. Nevertheless, the difference in blade structural rigidity caused a varying signal response during impact, which might have increased the possibility of error and requires careful data interpretation.

Continuing the previous study by Shin et al. [107], Jang et al. [113] utilized FBG sensors for the detection of impact damage location by employing grids in the area of interest on a composite structure. Four FBG sensors were multiplexed and attached to the inner surface of a 30-ply composite, with another 30-ply composite structure manufactured with six 10-ply stringers to emulate an aircraft wing structure. A round-headed impactor was then used to impart 1 J of energy on the composite samples. Eventually, a Neural-Network (NN) method was employed for data processing and optimization to determine the impact location. The study revealed that NN training could pinpoint the impact location to a certain accuracy as the maximum resultant error produced by NN training was smaller than the grid size (48.72 mm vs. 250.00 mm). In detecting damage severity due to impact, the wavelength pattern exhibited AE signals and sudden change in frequency portion, ascribed to the presence of fracture within the composite systems. The research group then applied the current finding to real-life applications by testing it on an Unmanned Aerial Vehicle (UAV) composite box wing structure [114], using six multiplexed FBG sensors compared to only four in their previous study [113]. Furthermore, they used an improved algorithm and sampling method to reduce errors, and the results were closely comparable between both studies.

Another impact triangulation method using FBG sensors was proposed by Sai et al. [115]. They employed FBG sensor arrays shaped into a right isosceles triangle on an 18-ply carbon/epoxy composite plate to detect impact events simulated using an impact hammer. By arranging six FBG sensors into two sets of right isosceles triangles, as shown in Figure 9, the impact source location could be theoretically triangulated by determining the difference between the elastic wave propagation time from the impact source and both sets of the FBG sensor arrays via the Morlet wavelet transform manipulation. Interestingly, it was discovered that errors produced (i.e., the difference between actual impact location and triangulated location) were higher when the impact source was closer to FBG arrays. This phenomenon was credited to the fact that as the impact source tends to get closer, the difference between the impact source and FBG arrays, D , and the distance between FBG in arrays, d , becomes smaller (refer to Figure 9). Subsequently, the elastic wave is no longer approximately equal to the plane wave, which was a fundamental assumption used for earlier calculations. Then, the authors further improved the method by employing several NN methods [116] and claimed that the impact source location detection obtained via NN, especially using Extreme Learning Machine (ELM), achieved an increased accuracy.

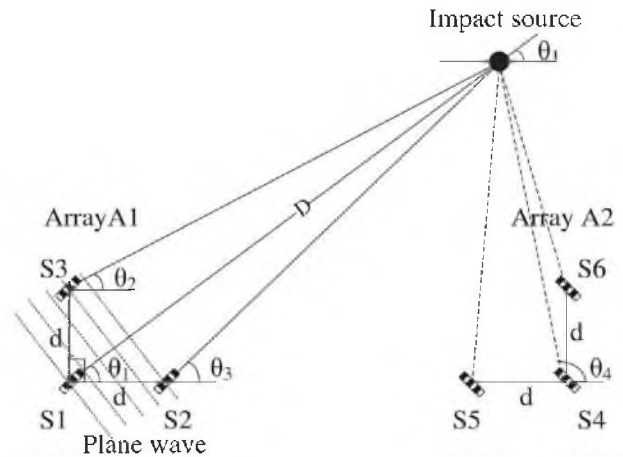


FIGURE 9. Formation of FBG arrays for the impact location triangulation [115].

In the other work, Raju et al. [117] investigated the feasibility of damage detection in the top-hat stiffener for offshore composite structures using an FBG sensor paired with AE as the signal source. The composite structure was manufactured via the vacuum infusion method using an 8-ply of glass fiber and vinyl ester as the resin. A single FBG acoustic sensor was attached on the web side of the top-hat structure by using ultrasonic couplant gel, similar to the ones portrayed in Figure 8. The compressive load was applied to the structure at 2 mm/min until reaching the fracture point, and the AE signal patterns were then analyzed via the transient and parametric analysis methods. Both results from the piezoelectric and FBG exhibited similar trends, although different in value, where each signal pattern could be ascribed to various failure modes, such as crack initiation, crack propagation, delamination, and fiber pullout. As a follow-up to the first phase of another study mentioned earlier [98], an FBG was attached to the flat surface of a manufactured composite specimen web to verify AE detection and applied with tensile load until fracture. The study revealed that the AE-FBG sensor could detect the corresponding damage occurring within the composite system as the experiment progressed. However, the amplitude values were lower than that of piezoelectric. The result was relatively comparable with another work by the same research group [118] with the fiber embedded inside the composite structure.

Kim et al. [119] performed a low-velocity impact damage assessment and strain monitoring on a cylindrical composite structure using a tin-coated FBG sensor. Several pairs of regular and tin-coated FBG sensors were attached 15 mm and 20 mm from the expected impact points on the filament-wound carbon/epoxy composite cylinder's outer surface. Different impact loads were then applied to the composite structure. It was reported that both types of sensors were able to detect initial failures in the composite structure, which were identified as matrix cracking and delamination, denoted by the sudden drop in strain detected as the applied load

progressed. Tin-coated FBG sensor also exhibited a higher stress transfer rate than the regular-coated one, possibly due to the shear-lag effect from the increased stiffness. The results also signify an enhanced sensitivity by the tin-coated FBGs but only at a lower impact load. The augment gradually decreased as the impact energy increased and became indistinguishable beyond the delamination point. The authors also demonstrated that the permanent deformation in the tin-coating imparted residual strain in the composite structure, with the highest being -0.00894% for 40 J of impact energy and 15 mm for the impact point.

Sun et al. [110] proposed the usage of FBG as a crack detection sensor in composite materials. FBG was attached to the surface of angle-ply laminates of various thicknesses prior to being subjected to tensile load. It was revealed that FBG wavelength shift and pattern highly correlated with the crack density that appeared on the composites. As the load was continuously applied to the specimen prior to crack nucleation, a proportional central peak wavelength shift is observed. FBG spectrum distorts and tends to widen as the crack starts to form, with the formation of minor peak wavelengths observed. As crack density increases, the minor, secondary peak wavelengths split from its primary peak central wavelength. At higher crack density, the FBG spectrum regressed to its typical undamaged laminate spectrum, with a marginal difference in the wavelength pattern. Interestingly, the FBG attached to the top surface of the specimen could detect crack formation on the bottom surface, proving the feasibility of attaching the FBG sensor to the exterior surface of the specimens. However, the authors anticipated that such conditions are only valid until a certain level of laminate thickness.

B. MECHANICAL AND THERMAL CHARACTERIZATION

Similar to embedded FBG, mechanical and temperature characterizations of laminate composites could be carried out by externally mounting the OFS. Although this review paper has presented multiple reports that embedded FBG composite laminates for characterization, some applications strictly inhibit OFS from being embedded due to various limitations. For instance, Pran et al. [105] conducted a long-term test of tension in bolted-joint composite structures due to creep using two FBG sensors. A 3 mm hole was drilled on a 60 mm thick glass fiber reinforced composite laminate, and two FBG sensors were inserted into the hole. One FBG was positioned near the midplane of the laminate, while the other was closer to the surface. Another hole was drilled to fit an M20 bolt, with thick steel bushings in between, and tightened with a suitable nut. Likewise, a 3 mm hole was drilled through the bolt to place an FBG sensor. Test specimens were then stored under different ambient conditions. Specifically, two specimens were exposed to ambient air conditions, while another two were placed in freshwater at room temperature conditions. The experiment was conducted for one whole year, and after one year, the nuts in one of the specimens from both conditions were tightened to their initial strain level. The

FBG detected a reduction in compression in the specimen plates one hour into the experiment, which was not reflected by the change in strain in the bolt. The finding was ascribed to the localized creep experienced by the glass fibers.

Rao et al. [104] utilized FBG as part of a strain and temperature sensing system in 3D-braided composite materials. The FBG was connected to an EFPI and placed in capillary quartz tubing prior to being mounted onto a 3D-braided carbon fiber composite manufactured via RTM. The specimens were then subjected to tensile and thermal load to study the strain and temperature response of the in-tandem optical fiber sensing system. The optical fiber sensing system detected strain well, as verified via an electrical strain gauge attached near the EFPI. Peculiarly, spectral distortion was observed for the FBG during the temperature sensing experiment. As the temperature decreased, the peak position slightly offset to its side. The non-symmetric spectral distortion was due to the periodic modulation of EFPI, represented by the third term in Equation 8:

$$\frac{I_{total}}{I_o} = \alpha_F \alpha_B R(\lambda) + \alpha_F \alpha_B R_f T(\lambda)^2 + \alpha_B R_f B S(\lambda) T(\lambda)^2 \cos \cos(2kd) \quad (8)$$

where I_o is the incident light source intensity, α_F and α_B are the forward and backward direction fiber couplers' coupling coefficients, respectively, $R(\lambda)$ refers to the reflectivity of the FBG, R_f denotes the reflectivity of the fiber end, $T(\lambda)$ is the transmittivity of the FBG, B represents the fringe visibility of the EFPI, k signifies the wave number, $S(\lambda)$ is the light source spectral profile, and d is assigned to the absolute length of EFPI cavity, which was analytically proven by the authors. It was postulated that using FBG with higher reflectivity could address this issue. Another simple method proposed to cater to this spectral anomaly was to accurately determine the peak in advance, achievable using the mean value of two wavelengths, specifically at a 3 dB level where the reading was stable. This method was proven to improve the temperature sensing accuracy, which enabled more accurate temperature-compensating strain measurement. The authors also claimed that the thermally-induced strain imposed on the OFS was mainly introduced by the resin, as carbon fibers are generally non-temperature-reliant.

On the other hand, Mizutani et al. [120] explored the in-situ strain monitoring of a liquid hydrogen cryogenic tank mounted on a reusable rocket using an FBG sensor. A UV-cured resin-coated FBG was attached to the exterior surface of a 10-ply carbon-epoxy unidirectional laminate using polyurethane (PU) adhesive. Preliminary studies revealed that the load applied on the composite tank under cryogenic temperature (approximately -150 °C) triggered the crack formation when the epoxy was used as adhesive for the FBG. This, in turn, caused irregular perturbation in the FBG wavelength due to the non-uniform strain distribution in the vicinity of the cracks and may subsequently cause inaccurate data interpretation. While readings from the FBG largely agreed with that of the strain gauge set as the reference sensor

during actual testing, a distinguishably significant noise was detected in one segment of the test, and the authors associated this with the insulation effect of the cryogenic tank.

Wei et al. [121] developed and demonstrated a high-pressure sensor by combining FBG with an anisotropic composite structure. The FBG was attached extrinsically using epoxy resin on the side of the carbon fiber-based composite structure with a total fiber volume fraction of 50%. The pressure sensing capabilities of the pressure sensor were characterized by placing it inside a pressure chamber. Another FBG was placed inside a tube and put together inside the pressure chamber as a temperature sensor. The FBG wavelength shift behaved as anticipated as the pressure inside the test chamber changed, although a temperature change was also detected. A temperature-compensated pressure value can be achieved using the wavelength shift value from the encapsulated FBG. Song et al. [106] reported another study on the feasibility of using FBG as a pressure sensor by housing it in a composite shell. An FBG was enclosed inside a filament-wound carbon/epoxy composite shell, with its end sealed securely by bonding cylindrical iron caps. The FBG-based pressure sensor was then placed inside a sealed chamber, where water at a known and controlled pressure was pumped into. The FBG wavelength shift with a change in the internal pressure of the test chamber depicted a linear relationship, which indicated a sensitivity value of 0.452 nm/MPa, which is well-agreed with the attached pressure regulator. The enclosed FBG sensor also showed good repeatability. However, a discrepancy was detected between the calculated and experimental value of pressure sensitivity, owing to the difference between the actual and calculated value of Young's modulus and Poisson's ratio, apart from any manufacturing imperfections.

Fernández et al. [103] assessed an SHM on a commercial airplane CFRP cockpit structure and CFRP-stiffened concrete pillars using FBG as sensors. A full-scale aircraft cockpit was manufactured using carbon fiber with 24 sets of FBG sensors securely positioned at various critical locations of the structure (Figure 10). Additionally, two sets of FBG and strain gauges were attached on the external surface of the concrete pillar consisting of a steel-reinforced concrete wound with carbon/epoxy composite via filament winding technique. These aeronautical and civil engineering composite structures were tested under several conditions. Accordingly, fluctuating discrepancies between the FBG and strain gauge sensor measurements were observed for the CFRP cockpit analysis. Some readings were also significant to even change the signs from tensile to compressive or vice versa. The authors ascribed the phenomenon to the inaccessible location between the FBG and strain gauge sensors or the manufacturer's restrictions. In contrast, the CFRP-reinforced concrete pillar exhibited significant discrepancy between FBG sensors during the initial stage of compressive loading due to insufficient parallelism between the test specimen and the pillar support, suggesting the remarkable capability of the FBG sensor to detect these experimental setup defects. Several

FBG fiber breakages were reported when the load applied exceeded the threshold value.

Cao et al. [16] employed quasi-distributed FBG sensors to examine the brittle fracture phenomenon in composite insulators' power transmission systems. Following the test method specifications, the tubular-shaped test specimens were made of GFRPs via the pultrusion method. Five FBG sensors were written, with each sensor attached to the outside surface of the composite insulator at 120° from each other about the centroid of the specimen's diameter. Specimens were submerged inside a container with nitric acid of known concentration prior to being applied with tensile load until fracture. The results revealed that the FBG wavelength shift was directly related to the number of cracks near the vicinity of the FBG sensor and the severity of the crack itself. The authors also reported several damaged FBGs throughout the fracture monitoring processes, which could be due to the tensile load applied surpassing the stress limit of the FBG material and possibly further worsened by the nitric acid corroding the sensors. However, such claims were never explicitly mentioned in the article.

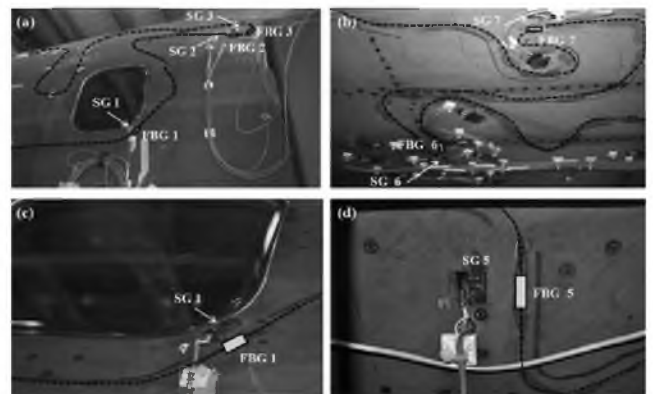


FIGURE 10. Images of the FBG and strain gauge installations on the commercial aircraft cockpit structure [103].

VI. COMPARISON BETWEEN EMBEDDED AND SURFACE-MOUNTED FBG

So far, this paper has reviewed several past literature studies focusing on both embedded and surface-mounted FBG. However, the deployment methods between these two sensors could not be directly compared since the composite laminates were made from different materials and manufactured with varying numbers of plies, the FBG locations were incomparable, and the sensing parameters were different. Geng et al. [122] are the only researchers that directly compared embedded and surface-mounted FBG, specifically the curing, temperature, static loading, and dynamic loading sensing capability between externally-mounted FBG and embedded FBG in composite laminate structures. The test specimens comprised a 22-ply carbon/epoxy laminate manufactured via the hot press method. One FBG was embedded between the 3rd and 4th ply, while the reinforcing fibers in both layers and optical fiber were positioned in a longitudinal

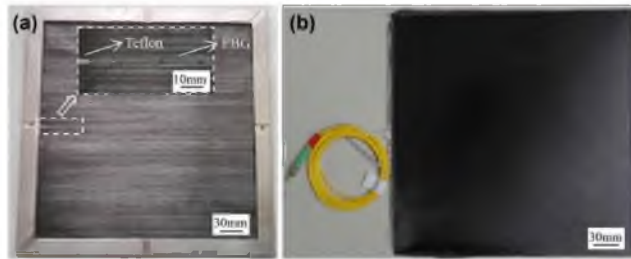


FIGURE 11. Image of the CFRP (a) before curing [122] and (b) after curing [122]. Notice that the FBG egress is protected by a layer of Teflon in the inset image.

direction. Another two FBGs were attached using epoxy, each on the top and bottom surface of the cured composite specimen, in the same coordinate as the embedded FBG. The image of the specimen before and after the curing process is shown in Figures 11(a) and 11(b), respectively. It was revealed that the post-curing FBG spectrum showed no spectral distortion, indicating its sensing reliability. However, the wavelength peak shifted to a lower value which dictates the presence of thermal residual stress due to curing. In addition, the temperature measured by the internal FBG accurately matched those of the surface-mounted FBGs and the actual set temperature.

During static loading test, weights were placed at several locations on the composite specimen and along the FBG's longitudinal axis to represent load. Accordingly, the wavelength shift in the FBG spectra linearly correlates with the load applied on the specimen, although the rate differed at each position. Despite being bonded perfectly symmetrical on the top and bottom of the specimen, the FBG spectra wavelength change under static loading was not completely symmetrical. This is due to the different individual ply thicknesses, which, when stacked, could minutely cause a difference in distance from the composite's neutral axis and, subsequently, marginally different exerted strain under static loading. Dynamic loading tests were carried out on similar coordinates to static loading. Based on the results, embedded FBGs exhibited slightly lower sensitivity to impact load than surface-mounted FBGs. The authors postulated that due to the stacking sequence, the impact load had dissipated as it propagated through the specimen thickness, causing the embedded sensor to detect less strain. The authors also argued that the impact response sensed by the FBG was similar regardless of the impact location.

Based on the literature reviews, it is evident that the intended application of the sensor itself is the main factor that determines whether the FBG sensor should be embedded or attached to the surface of the composite laminates. While past work by Freire et al. [99] and Prusty and Raju [98] utilized both FBG sensors, no direct comparisons were made concerning their sensitivity or reliability. Nevertheless, both works have practically endorsed the suitability of embedded and surface-mounted FBGs as sensors. Conversely, Geng et al. [122] directly compared the two optical fiber

conditions and concluded that embedded and surface-attached FBGs are highly capable sensors. The authors also stated that both sensors demonstrated noticeable differences in sensitivity, specifically during static and dynamic loading tests. However, such outcomes were already anticipated since both loading tests arguably remained under the influence of the specimens' geometrical effect to a certain degree.

Both deployment methods possess unique and distinct characteristics, as listed in the performance comparison in Table 4. The list shows that embedded FBG sensors specifically monitor interlaminar strain and the interlaminar temperature, which is possible because they are embedded between the fiber layers. The close proximity of the embedded sensor to the damage location gives it advantages in terms of capturing the strain and acoustic signatures released during failure events. Meanwhile, the surface-mounted technique is only capable of measuring surface strain, and these parameters also give the possibility of detecting damage. The embedded technique is less flexible and requires careful planning as the sensor position is permanent after the FRP manufacturing process is completed. On the other hand, surface-mounted FBGs are more flexible, require less complex installation and maintenance, and can be deployed immediately to a desirable structure. Surface-mounted FBGs are more likely to be affected by human and environmental perturbations. In the case of sensor damage or breakage, embedded FBGs are susceptible to damage during manufacturing if the optical fiber is not handled carefully. Both embedded and surface-mounted FBGs are vulnerable to in-service damage. Excessive loading impacted on the host structure could also result in damage to embedded FBG; thus, study of the structure to identify the strategic position is required, especially for complex FRP composite structures. The performance of embedded FBGs can be affected by other issues, such as resin-rich areas, nestled FBG inside the reinforcing fibers, chirped FBG sensor grating, angular and axial angular disorientation of FBG, fiber debonding and delamination, and additional residual strain, which could significantly affect the sensing capabilities of the FBG or the mechanical integrity of the host composite laminate, or even both. More in-depth elaboration regarding these issues is provided in Section IX of this paper. Therefore, careful consideration and planning should be conducted before deciding on the incorporation method of the FBG into the FRP laminates, especially on the intended sensor application.

VII. IN-COMPOSITE FBG SENSOR CHARACTERIZATION

Another essential aspect of FBG embedment in composite laminates is the characterization of the FBG itself. In this subsection, several past literature studies on the evaluation and/or characterization of new FBG materials or sensor enhancement techniques and the impact of these novel materials or techniques on the sensitivity of the FBG are presented. As opposed to characterizing its host polymer, FBG is commonly embedded inside composite materials to determine its sensing capabilities. Utilization of novel FBG material

TABLE 4. Performance comparison between embedded and surface-mounted FBG on composite laminates.

	Embedded	Surface-mounted
Main characteristics	<ul style="list-style-type: none"> - FBG sensor incorporated between reinforcement fibers layers during the manufacturing process - Permanently embedded inside the composite laminate <p>Usually utilized for smart composites</p>	<ul style="list-style-type: none"> - Composite laminates are manufactured first prior to attaching FBG securely on the cured composite laminate surface using high-performance adhesive
Intended sensing application	<ul style="list-style-type: none"> - Internal composite strain and temperature state during the curing stage - BVD detection and localization 	<ul style="list-style-type: none"> - Damage detection and localization - SHM for large structures
Detected physical parameters	<ul style="list-style-type: none"> - Interlaminar strain, interlaminar temperature, impact, vibration, and damage 	<ul style="list-style-type: none"> - Surface strain, surface temperature, impact, damage, vibration, and pressure
Manufacturing technique	<ul style="list-style-type: none"> - Pre-strained FBG fixed between selected layers of the composite laminate prior to resin impregnation or curing - The laminate fabrication process may include hand lay-up, hot press, VARIM, Vacuum-assisted Resin Transfer Mold (VARTM), vacuum bagging, and autoclave curing 	<ul style="list-style-type: none"> - Pre-strained FBG attached to the surface of cured composite laminate using adhesives or the composite's matrix epoxy - The laminate fabrication process may include hand lay-up, hot press, VARIM, VARTM, vacuum bagging, and autoclave curing
Temperature susceptibility	<ul style="list-style-type: none"> - Sensitive to detecting curing/chemical reaction temperature shift - May be influenced by the temperature change of certain fiber or matrix 	<ul style="list-style-type: none"> - Prone to sensing external/ambient/environmental temperature perturbation - May lead to inaccurate sensing
Strain susceptibility	<ul style="list-style-type: none"> - May be influenced by thermal-induced strain due to chemical reactions or curing cycle - More sensitive in detecting strain perturbation on its axial orientation compared to transversal strain 	<ul style="list-style-type: none"> - Heightened sensitivity due to surface measurement, which might not be representative of the actual value
Risk of sensor damage	<ul style="list-style-type: none"> - Prone to breakage during manufacturing - Sensor damage/breakage dependent on host composites' fracture strength 	<ul style="list-style-type: none"> - Less susceptible to damage during sensor placement - Prone to in-service breakage due to external factors - Usually requires additional protection coating
Maintenance	<ul style="list-style-type: none"> - Impossible for physical maintenance and replacement - Requires replacing the whole smart composite structure 	<ul style="list-style-type: none"> - Possible sensor replacement and maintenance - Capable of visual inspection/confirmation
Laminate-related defects	<ul style="list-style-type: none"> - Resin-rich region/air pockets - Debonding - Reduced mechanical properties 	<ul style="list-style-type: none"> - Nothing significant
Sensor-related defects	<ul style="list-style-type: none"> - 'Nestled' FBG - Chirped grating - FBG angular rotation and orientation shift - Residual strain due to cure-shrinkage/laminate warpage 	<ul style="list-style-type: none"> - Nothing significant

or microstructure, or even a novel sensitivity-enhancement method, requires the FBG to be embedded to observe its behavior inside the polymeric composite laminate and how they affect the host composite microstructure and mechanical properties. In fact, novel FBGs' performance is occasionally set as a benchmark to compare with other types of embedded OFSs.

Previously, Ramakrishnan et al. [123] proposed using polarimetric sensors and FBG for simultaneous multiparameter measurement in laminate composites. Individual FBG, acrylate-coated Polarization Maintaining Photonic Crystal Fiber (PM-PCF), and stripped PM-PCF were embedded just below the surface of an 8-ply unidirectional E-glass/polyester composite, and subjected to thermal and flexural load to observe strain, temperature, and thermally-induced strain sensing capabilities of each OFS. During the three-point bending experiment for strain-sensing, the FBG exhibited a sensitivity of $0.0862 \text{ dB}/\mu\epsilon$, followed by the coated and stripped PM-PCF at $0.00464 \text{ dB}/\mu\epsilon$ and $0.00467 \text{ dB}/\mu\epsilon$, respectively. The authors found that the buffer coating on the FBG significantly reduced the effect of thermally induced strain. For thermally-induced strain measurement, the FBG showed the highest sensitivity at $0.0845 \text{ dB}/\mu\epsilon$, followed by the stripped PCF at $0.00462 \text{ dB}/\mu\epsilon$ and coated PCF at $0.000464 \text{ dB}/\mu\epsilon$. Therefore, the authors have chosen stripped PCF as a sensor for thermally-induced strain.

Rajan et al. [124] also evaluated and compared the performance of FBG as a sensor in composite materials against polarimetric based sensors. Panda fiber and PM-PCF were embedded inside an 8-ply of carbon/epoxy and glass/epoxy laminate with the sensors embedded just below the surface of the laminate. During strain measurement, the FBG exhibited marginally higher sensitivity compared to PM-PCF. For the case of temperature sensing, the embedded FBG showed a higher sensitivity compared to its free-space sensitivity, owing to the birefringence effect from the composite materials' thermal expansion. This also explains the relatively unchanged temperature sensitivity of the FBG upon being embedded inside the CFRPs compared to normal, free-space temperature sensitivity, as carbon fiber possessed a smaller thermal expansion coefficient than glass fiber. A similar observation was also present in the case of different FBG coatings, where acrylate-coated FBG depicted a higher sensitivity compared to polyimide-coated FBG. While both PM-PCF and FBG were able to measure the applied vibration frequency to a certain degree adequately, the FBG could only detect vibrations with an amplitude larger than 0.3 mm compared to the minimum 0.1 mm detectability by the PCF.

Following the previous study, the research group carried out an extended study emphasizing low-frequency dynamic loading sensing using FBG and PM-PCF [125]. Both FBG and PM-PCF were embedded between the 2nd and 3rd layer of an 8-ply glass/polyester unidirectional laminate manufactured via the hand lay-up method. Prior to being embedded, both optical fibers were applied with pre-strain by fixing

both fibers' ends. In the vibration sensing test, the measured periodic wavelength change of the FBG spectra showed a lower effective noise content than that of PM-PCF, as the FBG was measured in the wavelength domain, as opposed to the intensity domain for the PCF measurement. Although the FBG spectra exhibited a noticeable harmonic distortion, the authors claimed that the FBG could resolve more significant details in harmonic contents.

In another study, Rajan et al. [71] fabricated Polymer-based FBG (PFBG) and utilized it as a sensor in composite laminates. The PFBG was produced using poly(methyl methacrylate) (PMMA) via the phase mask technique. Besides standard FBG, PFBG was embedded between the 2nd and 3rd layer of an 8-ply unidirectional glass/polyester, and the cured composite laminates were characterized for their thermal and flexural response. It is worth noting that during the embedding stage of both FBGs, the firmly attached optical fibers on the glass fiber layer caused pre-straining and potentially residual strain post-curing since the FBG showed spectral peak-broadening compared to its free-state spectrum. It was highly plausible that the phenomenon was related to the inhomogeneous strain distribution on the FBG sensor gratings. Another interesting observation was that only a portion of the PFBG consisted of polymer-based optical fibers, while the rest was composed of single-mode silica fiber pigtail attached to the polymer fiber via UV-cured adhesive. It was believed that the adhesive between the silica/polymer interface might have caused noise on the reflected spectra in the form of ripples, as no such occurrence was exhibited for the standard silica FBG. During the thermal characterization test, PFBG exhibited spectral broadening instead of spectral shift, as shown by the silica FBG. PFBG also depicted a negative wavelength shift gradient due to its negative thermo-optic coefficient. Nevertheless, both embedded and free-space sensitive PFBGs were marginally similar. The authors theorized that this was due to the inefficient longitudinal thermal strain transfer of the PFBG gratings. On further investigation, PFBG reacted to transverse thermal strain more adeptly, possibly owing to the absence of coating on the PFBG, which subsequently caused a direct transfer of any surrounding perturbation to the sensor core. In the flexural response sensing, although both PFBG and silica FBG showed no spectral broadening or distortions, PFBG recorded a slightly inaccurate strain, which was attributed to the inefficient transfer of mechanical strain due to the difference in properties between the PFBG and polymer composite materials.

Zhan et al. [126] also focused on utilizing PFBG as a multiparameter sensor inside a thermoplastic composite laminate. Polyimide was chosen as the material to fabricate the FBG, and the PFBG was embedded inside a carbon/polyphenylene sulfide (PPS) during the AFP process with a 0° and 15° angle to its longitudinal axis. The strain and temperature changes throughout the manufacturing and curing process were monitored. The authors postulated that the PFBG temperature sensitivity varied greatly due to a significant mismatch of

thermal expansion coefficients between the resin and optical fiber. Therefore, the Bragg wavelength shift should be represented as:

$$\Delta\lambda_B = \lambda_B [\alpha_f + \xi + (1 - P_e)(\alpha_{res} - \alpha_f)] \Delta T \quad (9)$$

where ξ is the thermos-optic coefficient, P_e represents the photo-elastic coefficient, α_{res} and α_f are the thermal expansion coefficient of the resin matrix and optical fiber, respectively, and ΔT denotes temperature change. According to the results, the FBG displayed a sharp peak intensity increase when the AFP roller passed through the region where the FBG was embedded due to the force exerted by the roller, besides an additional force imposed during the fiber ply placement and the temperature change. These additional perturbances subsequently caused the emergence of side lobes on the spectra. It is also interesting to note that while the composite plies were heated to 250 °C prior to being placed down, the highest temperature detected by the FBG was only up to 231 °C. Naturally, as more layers are laid-up, the temperature reading drops. Hence, the authors credited this phenomenon to the heat loss due to the conduction between layers.

Meanwhile, Luyckx et al. [67] evaluated the influence of material and geometrical birefringence of FBG by embedding both types of fiber sensors in composite laminates. The first FBG sensor was manufactured by inscribing Bragg gratings on a bow-tie fiber (geometrical birefringence), while the other was on a highly-birefringent microstructured optical fiber (material birefringence). The sensors were embedded between the 2nd and 3rd layers of a 16-ply carbon/epoxy composite laminate, and the specimens were loaded with bending, transversal strain, and thermal load. While both geometrical and material birefringent FBGs showed marginally similar sensitivities during the flexural test, the same could not be said during the transversal strain test. The bow-tie FBG showed a higher sensitivity, which was thought partially owed to its thinner cladding.

Interestingly, both FBG sensors showed significant differences during the thermal-cooling test, in which the bow-tie FBG exhibited a substantially higher sensitivity (0.42 pm/°C) as opposed to 0.026 pm/°C for the microstructured FBG. The authors associated this finding with the difference in material and geometrical birefringence of both types of FBG, with the former being more inherently temperature-reliant for bow-tie FBG. Focusing on the birefringence of FBG, the authors utilized residual strain-induced birefringent FBG as a multi-axial sensor in composite laminates in another study [126]. The study employed two types of FBG sensor settings: one type of sensor comprised of FBG encapsulated inside capillary fused silica tubing to measure pure axial strain, while another was non-encapsulated FBG with its coating stripped to measure the total strain exerted on the sensor gratings. Both sensors were separately embedded on the neutral plane of a 16-ply cross-ply carbon/epoxy laminate, as depicted in Figures 12(a) and 12(b), respectively, and loaded with longitudinal and transversal in-plane tensile load, as well as out-of-plane transversal load. The effect of

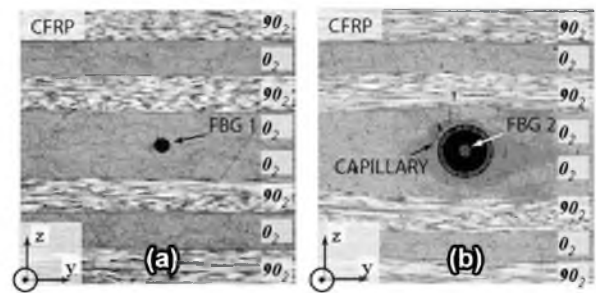


FIGURE 12. The cross-sectional profile of the (a) coating-stripped FBG, and (b) FBG inside the capillary glass tube embedded in the cross-ply laminate [127].

transverse strain during the applied longitudinal load was revealed to be marginal. However, during longitudinal load testing, the transverse in-plane strain component exhibited higher reading variations than its longitudinal counterpart, indicating that the transversal strain in optical fibers was closely related to changes in its axial wavelength shift. This claim was also valid in terms of error – a small error in axial strain detection ($\sim 1\%$) led to a more considerable error in the transverse strain direction ($\sim 13\%$). After applying the transversal load, both stripped and encapsulated FBG showed almost 20 times smaller wavelength shifts relative to the longitudinal load case; even for the out-of-plane transversal load case, the FBG could still detect strain changes in the complementary axes' direction.

Wang et al. [6] attempted to improve the FBG sensitivity in composite materials using fiber buffer coating. Three individual FBGs positioned at 0°, 45°, and 90° to the longitudinal axis of the reinforcing fiber were embedded between the 7th and 8th layer of a 24-ply carbon/epoxy laminate prior to being cured and characterized for the flexural and thermal response. In a preliminary study, the simulation and experimental outcomes demonstrated the effect of buffer coating on FBG under three conditions: standard FBG, coating-stripped FBG, and recoated FBG. The stripped FBG showed the highest birefringence effect with peak splitting on its reflectance wavelength spectrum, while the standard FBG showed slight spectral distortion, and no discernible spectral anomaly could be detected for recoated FBG. The addition of an extra thickness of coating enveloping the sensor grating was also thought to mitigate the birefringence of the FBG by balancing the longitudinal and transversal stress component imposed on the sensor. The recoated FBG also showed remarkable temperature sensing capability after being embedded inside the composite material, recording a sensitivity of 13.33 pm/°C and 14.46 pm/°C at 0° and 90° oriented FBG sensors, respectively. Nonetheless, the study did not elaborate on the higher sensitivity for the perpendicularly-placed sensor. On the other hand, the 0° oriented FBG sensor exhibited the highest strain sensitivity under applied flexural loading, as it was parallel with the axial tensile stress exerted due to the deformation of the composite material. It was also noted that as load

increased during the flexural test, the wavelength spectrum of the FBG exhibited slight spectral distortion in the form of spectral broadening, highly suggestive of non-uniform strain distribution along the sensor grating.

VIII. RECOMMENDATION ON FBG EMBEDDING CONDITIONS AND TECHNIQUES

After reviewing numerous works utilizing embedded FBG inside fiber-reinforced polymer composite laminates, this section lists several ideal optical fiber embedding conditions and techniques to obtain defect-free specimens with defect-free sensing capabilities. Note that these proposed ideal embedding conditions and techniques serve more as precautions – matters requiring extensive consideration, careful planning and strategy, and utmost care during or prior to the embedment process. These proposed conditions and techniques are also mainly based on the various issues, observations, problems, and findings discussed in past papers. Also, discussion on ideal techniques for surface-attaching FBG is not included due to the almost non-existent problems reported in past literature related to the surface-attachment process.

A. APPLICATION OF PRE-STRAIN TO STRAIGHTEN FBG

One of the essential precautions during the FBG embedding procedure is to ensure that the OFS is perfectly straight and aligned to increase the reflectivity of the FBG. This is achievable by fixing both ends of the FBG with adhesive tape during its placement between the composite laminate layers prior to resin impregnation so that the OFS remains securely straight throughout the curing process. It is also advisable to avoid fixing the FBG end using adhesive tape on the composite ply itself since it may block resin impregnation into the reinforcement fiber plies within that vicinity. The tape may also act as a defect and, consequently, as a stress concentrator. Instead, the adhesive tape should be placed on the preparation surface area at the edge of the specimen. Several past works have utilized this method [71], [95], [124], [126]. It is also worth noting that excessively fixing the FBG may introduce pre-strain onto the sensor, which in turn may induce additional residual strain post-curing, as reported previously [86]. Therefore, special care must be taken to avoid introducing pre-strain onto the sensor.

B. PROPER FBG AXIAL AND ANGULAR ORIENTATION

Apart from ensuring the FBG remains straight, it is also crucial to ensure that the OFSs are correctly axially and angularly oriented during the embedding and specimen manufacturing process. It was previously shown that strain detected by the FBG dropped as the embedding angle deviated from the longitudinal axis of the reinforcing fiber [65]. For the case of geometrically-birefringent FBGs, including bow-tie fiber, Panda fiber, or any other novel microstructures, such as the one designed by Sulejmani et al. [69], [128], the optical fiber angular orientation must be appropriately aligned. Any misalignment may cause a drop in sensitivity, as

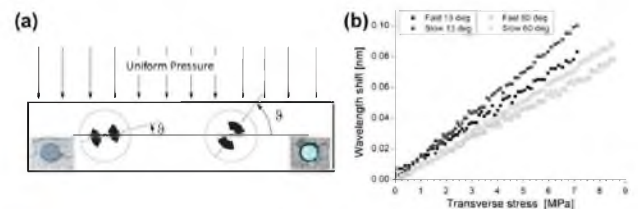


FIGURE 13. (a) The cross-sectional image of the angular misalignment of a highly-birefringent OFS and (b) the corresponding wavelength shift with applied uniform load [127]. Notice the difference in wavelength shift as the misalignment angle increases.

portrayed by the in-composite cross-section illustration in Figure 13(a) and its corresponding wavelength shift upon applied uniform strain in Figure 13(b).

C. INGRESS AND EGRESS POSITION/PROTECTION

During the FBG embedding stage, the ingress and egress locations (the optical fiber enters and exits the composite laminate) are the weakest. The FBGs are prone to damage or breakage at these locations, usually due to the sharp edges of cured polymers. Therefore, the most straightforward approach in addressing this issue is by providing ample protection to the FBG at these locations by simply enclosing the protruding optical fibers in protection sleeves made up of rubber, Teflon, or steel, as demonstrated by past researchers [7], [129], [130]. Another feasible method is to use a detachable connector system, as proposed by Basile et al. [131] and Tsutsui et al. [132]. Details regarding this alternative method are discussed in Sub-Section IX-F.

D. PROPER FBG CARE DURING MANUFACTURING

It is not an understatement to say that FBG is a highly fragile sensor. As such, proper care must be taken during its embedding process and not just on its ingress/egress position, as discussed earlier. Similarly, the optical fiber must not be under excessive bending load or bending curvature, especially during the experimental system setup requiring the OFSs to be connected to multiple ports and places. This indicates that the experimental setup must be planned ahead, even during the manufacturing process of the composite specimen. Apart from this, some manufacturing processes of the in-composite embedded FBG, such as autoclave curing, including exposing the specimen to considerable pressure cycles, which could physically damage the optical fiber during the specimen manufacturing stage.

E. PROPER PLANNING FOR FBG WAVELENGTH, NUMBER, LENGTH, AND LOCATION

The planning stage is the most important stage of FBG embedment in FRP composite laminates. The planning includes designing the OFS – length of gratings, number of gratings, optical fiber materials, the distance between gratings, splicing or multiplexed, sensor amount per optical fiber, and use of capillary tubes – as well as planning its

placement – optimized location, and the number of FBGs per composite ply. These multitudes of factors may influence the overall outcome of the FBG sensor. Therefore, it is not surprising to discover that most researchers opted for simulations prior to carrying out experimental works, such as that reported by Tsamasphyros et al. [133], who conducted a numerical simulation to achieve the optimized embedment placement of FBG inside composite laminates. For applications requiring multiple FBGs, it is crucial to plan and deploy the FBGs with distinct differences in the peak wavelength values. This is to ease the process of data interpretation and analysis. Conversely, similarly close peak wavelength valued FBG might hamper the data analysis stage, especially for analyzing simultaneous perturbations at different locations on the composite laminate specimens. Moreover, it is vital to estimate the wavelength shift and predict its direction to avoid spectral overlapping. This is achievable by performing

F. COATING AND CAPILLARY TUBE

Polymer-coated FBG is commonly available as the coating provides physical protection on the fragile structure of the OFS. Apart from the coating, FBGs are encapsulated in capillary tubes to cater to cross-sensitivity issues. However, the presence of polymer buffer coating might cause inefficient strain transfer on the sensor grating, as demonstrated by Khadka et al. [134], owing to low-quality bonding between the matrix and the polymer buffer coating. The author's group also proved that stripping the FBG bare of the buffer coating exhibited excellent interfacial bonding between the composite matrix and the FBG sensor, as shown in Figure 14. On the other hand, Wang et al. [6], [9] demonstrated that optimizing the coating thickness could mitigate the birefringence effect of the FBG by balancing the asymmetric strain distribution on the sensor grating. They showed that stripping the FBG bare led to wavelength distortion in the form of peak splitting due to non-uniform strain distribution on the sensor grating.

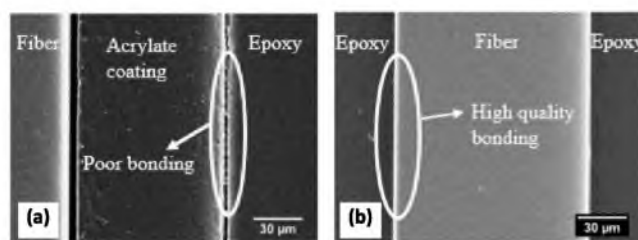


FIGURE 14. Microscopic imaging of the interfacial bonding between the FBG and polymer matrix for (a) unstripped FBG and (b) bare FBG [134].

IX. ISSUES AND CHALLENGES WITH FBG AS SENSORS

This paper has repeatedly demonstrated the reliability and capability of FBG to act as an individual or multiparameter sensor in fiber-reinforced composite laminates, regardless of whether it is surface-attached or embedded. Nevertheless, the OFS is imperfect and still prone to induce specific issues, which may adversely affect its host composite materials

and/or the sensing process itself. Hence, this sub-section highlights and addresses the following issues. First, the effects of FBG embedment on the mechanical properties of its host composites is explained, mainly on the deterioration of composite laminate properties due to the presence of FBG sensors inside the FRP microstructure. Following this issue, several defects on composite laminate microstructure that directly result from FBG embedment or imperfection during FRP manufacturing are presented. Subsequently, the discussion focuses on FBG failure due to in-service optical fiber fracture or during testing, followed by the cross-sensitivity issue of FBG – how it affects multiparameter sensing and how current researchers cope with it. Another issue deemed necessary to highlight is the limited sensing region of FBGs, or it only allows point sensing. Then, several strategies to manipulate this limitation into distributed or quasi-distributed sensing are presented. The discussion finally emphasized the methods to handle the precise location and placement of embedded FBG before stressing the limitation of FBG to act as sensors in other composite systems efficiently.

A. EFFECT OF FBG ON MECHANICAL PROPERTIES OF HOST COMPOSITES

Using the definition of composite materials [135], [136] as stated in the earlier parts of this paper, OFS is qualified to be considered as a reinforcement to an existing composite material upon its inclusion into the composite's microstructure. As such, it could be argued that embedding FBG into an FRP composite laminate will most definitely influence the output mechanical properties of the host composites. The issues are whether they are detrimental or beneficial and whether the effects are marginal or significantly distinguishable. The former could be easily solved – although FBG is mainly made of silica which is the similar main ingredient in reinforcing glass fibers, FBG was never intended as a load-carrying reinforcing fiber. In fact, to the best of the authors' knowledge, no available literature at the point of writing this paper has decisively shown that embedding FBGs enhanced the mechanical properties of its host composite laminates. This indicates that the inclusion of FBG inside composite laminates deteriorates its mechanical properties, but to what extent?

Past literature has shown mixed responses regarding the severity of the influence imparted by FBG on its host's mechanical properties. On the one hand, some researchers claimed that an apparent reduction in mechanical properties was observed due to FBG embedment. Papantoniou et al. [68] demonstrated a decrease of 300 MPa in ultimate tensile strength when FBG was embedded in the center of the specimen, with a further drop of 100 MPa observed when the optical fiber was placed off the center to a non-symmetrical axis. This was associated with the additional bending effect exerted by the optical fiber and manufacturing imperfection caused by the FBG, such as debonding. Furthermore, the size of FBG, which is often five to tenfold larger than individual reinforcing fibers, is also

thought to contribute to this issue, as they act as stress concentrators.

Some studies even concentrated on investigating the influence of FBG embedment on itself. For instance, Khadka et al. [134] studied the impact of FBG embedment on the mechanical properties of its host composite material. FBGs were embedded between particular layers of an 18-ply unidirectional carbon/epoxy composite, cured, and tested for their tensile response. The authors observed that the composite strength steadily deteriorates as the FBG is positioned farther from the middle ply of the composites (towards the outer plies). However, the effect was not reflected in its tensile modulus. Upon further investigation via the microscopic imaging method, it was discovered that due to the employed lay-up sequence, the FBG positioned towards the outer layer tends to get 'nestled' into its adjacent 0° ply, as similarly reported by another literature [95]. It was also apparent that the nestled FBG was not enveloped in epoxy resin, insinuating fiber debonding. To further test this theory, the authors embedded an FBG perpendicularly in a unidirectional carbon prepreg and discovered the presence of a resin-rich area surrounding the FBG. The authors, however, did not provide further information on how the resin-enriched area governs the microstructure and mechanical response of its host composite, not to mention how it can impact the sensing capability of FBG.

In contrast, other researchers argued that the FBG implanting effects were marginal and could even be considered negligible [107], [123]. For instance, Kuang et al. [95] claimed that the embedment of the optical fiber does not impart local perturbation in the vicinity of the FBG itself. The claim was further substantiated by showing that the FBG spectra of all unidirectional specimens depicted no spectral distortion, which observed no significant microstructural change on the region near the sensor, implying no major effect on the mechanical properties of the host composite laminates.

On top of FBG inclusion inside the composite laminate, the utilization of capillary tubes was another factor that may indirectly affect the laminate's mechanical properties. Previously, researchers often encapsulated their FBGs inside a capillary tube made from various materials to ensure that they would be in a constant strain-free state and protected from thermally-induced strain due to the cross-sensitivity issue of the FBG [62], [79], [82]. Again, the marked discrepancy between the diameter of the capillary tube and the reinforcing fiber (two to four times difference in size) may impose some perturbation in its vicinity microstructure, acting as a stress concentrator and subsequently altering the mechanical properties of the host laminates. This agrees with the claims made by past researchers [7], [20], [32], [67], although they were never proven with relevant scientific data or studies.

Also, note that this paper only covered the effects on mechanical properties of the composite laminates and not any other properties, such as thermal or fire response, since it is improbable that the embedment of FBG would impart any significant deterioration to these properties. The only other

aspect known to change due to FBG being embedded inside the composite laminates is its local microstructure, which is explained in the following sub-section.

B. EFFECT OF FBG ON THE MICROSTRUCTURE OF COMPOSITE LAMINATES

As mentioned earlier, FBG embedment inside the composite laminates is expected to distort the composite's microstructure. This distortion in the vicinity of OFS might contribute to the adverse effects imparted on the mechanical properties of the composite laminates. As the previous sub-section has already addressed the drop in properties, this sub-section focuses on the microstructure changes, which may lead to the deterioration in mechanical properties covered earlier.

The first crucial microstructure anomaly reported upon the inclusion of OFS into composite laminates is the emergence of the resin-rich region. This phenomenon was reported by various studies, among them by Song et al. [137], who reported the presence of spindle-like resin-rich enveloping the FBG when the optical fiber was placed transversely to the direction of the reinforcing fibers. A similar finding was observed by Minakuchi [83], who claimed that FBG embedment displaced and caused misalignment of reinforcing fiber, along with the presence of resin-rich region, as illustrated in Figure 25(a). The author added that the region imposed a limited effect on the sensing capability of the fiber. However, no further elaboration was given on its impact on the composite's mechanical properties.

Shivakumar et al. [138], [139] dedicated a study to explore further the effect of FBG embedment on the change in microstructure it caused to its surrounding region. FBG was embedded midplane of an 8-ply, 16-ply, and 20-ply unidirectional carbon/epoxy composite, with the optical fiber oriented at 0° , 30° , 45° , 60° , and 90° orientation. The manufactured specimens were then characterized for their morphological structures and tensile and compressive properties. It was revealed that except for the 0° FBG orientation, the optical fiber in all other orientations created a ply wave with resin pockets to fill them, which agrees with that of Minakuchi [83] and Song et al. [137]. It is also interesting to note the emergence of air pockets for the orientation at 60° and 90° , as shown in Figure 15(b). The study measured the disturbance angle—the opening angle of the end of the spindle-like resin-rich pocket—and the area of the resin-rich region and concluded that they were almost constant regardless of the FBG orientation inside the composite. Nevertheless, differences in value were still detected when comparing those obtained from 8-ply and 16-ply laminates, which the authors credited due to the manufacturing variation as more plies were added.

In the mechanical tensile test, the authors postulated the failure mechanism of the composite laminate under the influence of the disturbance caused by the embedded FBG, as illustrated in Figure 16(a). As the axial load progressed, the transverse stress concentrated at the end of the resin-rich

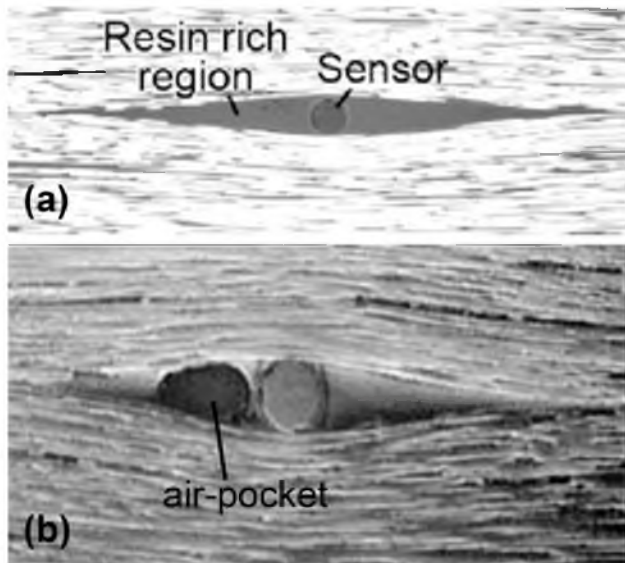


FIGURE 15. (a) Resin-rich region and fiber misalignment around the FBG, as depicted by Minakuchi [83], [82]; (b) The presence of air pocket in the resin-rich region for FBG orientation at 90° [138].

pocket due to the geometric perturbation. Failure was initiated with fiber-matrix debonding at the previously mentioned stress-concentrated region, which propagated with load, before stopping and failure due to breakage of the reinforcing fiber. As opposed to the tensile test findings, failure initiation was first detected by debonding at the FBG-matrix interface due to the concentrated transverse tensile stress, which then propagated to the resin pocket end, followed by fiber micro-buckling. The proposed failure mechanism is presented in Figure 16(b). Although the tensile strength dropped by a maximum of approximately 10%, which is considered minimal, the failure initiation stress was lower than the ultimate strength. Interestingly, compressive strength suffered a more significant drop of up to 40%, which is highly suggestive of the heavy reliance on compressive properties to the orientation of the OFS. Notably, all the maximum drops in properties were recorded by the 90° orientated FBG sensor.

Another critical microstructural defect caused by the FBG embedment occurred when the optical fiber was embedded in an adjacent unidirectional reinforcing fiber ply, leading the FBG to be nestled inside the fiber ply, as depicted in Figure 17. This phenomenon was observed in numerous studies. For instance, Shivakumar and Emmanwori [138] reported such observation upon embedding the fiber between two $0^\circ/0^\circ$ unidirectional plies. Conversely, Kuang et al. [95] observed FBG nestling upon using a $0^\circ/90^\circ$ unidirectional configuration, where the optical fiber submerged itself inside the adjacent 0° ply and possibly displaced by the 90° ply, as depicted in Figure 17. A similar finding was also claimed by Song et al. [137], who tested several lamina configurations, including $0^\circ/0^\circ$, $0^\circ/90^\circ$, and $90^\circ/90^\circ$. The authors concluded that the FBG will always be nestled when embedded adjacent to a longitudinally-parallel ply. Interestingly,

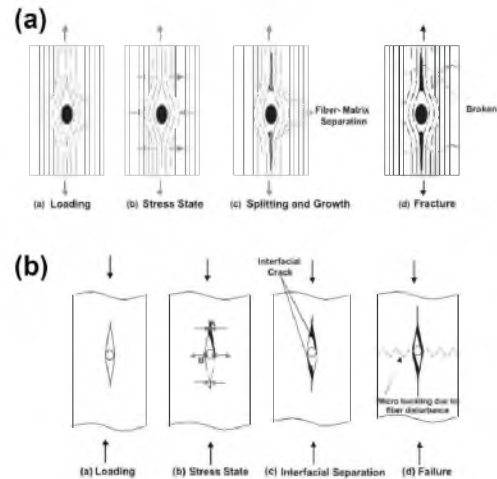


FIGURE 16. Microscopic imaging of the interfacial bonding between the FBG and polymer matrix for (a) unstripped FBG and (b) bare FBG [138].

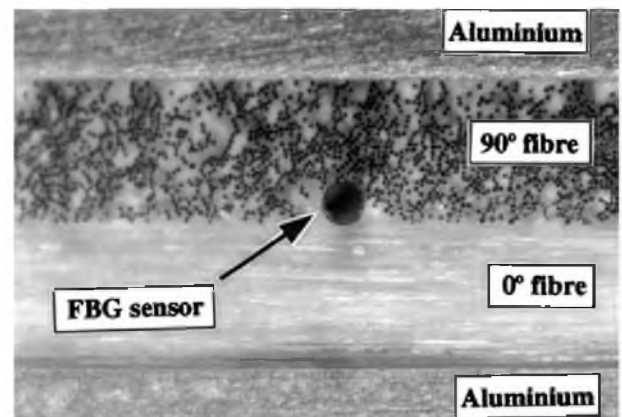


FIGURE 17. Microscopic imaging of the interfacial bonding between the FBG and polymer matrix for (a) unstripped FBG and (b) bare FBG [95].

Song et al. also mentioned that almost no resin enveloped the optical fiber in this condition, which might explain the failure mechanism and the drop in mechanical properties, as mentioned earlier. However, this could be due to material incompatibility or manufacturing imperfection. Kuang et al. [94], [95] also elaborated that the nestled FBG between the longitudinally-parallel reinforcing fibers was shielded from the radial compressive stress of the adjacent non-axis plies. However, radial compressive stress from the individual 90° reinforcing fibers could still be exerted should the optical fiber be incompletely nestled inside the 0° ply, as in the case depicted in Figure 17. This may induce non-uniform strain distribution on the sensor, which consequently induces FBG spectral distortion.

C. FBG FAILURE DUE TO BREAKAGE

Although FBGs are often incorporated in composite laminates and intended for NDTs, such as strain and temperature sensing or specific tests or applications progress

until the composite structure becomes fractured, the FBG is sometimes broken in the process. Several studies highlighted earlier have reported the failure of FBG. For example, Freire et al. [99] embedded several fibers inside a composite laminate to act as a ‘repair patch’ on a steel pipe. However, the FBGs failed under repeated hydrostatic tests after 10 cycles and reached $5\,000\ \mu\epsilon$. Fernández et al. [103] reported another FBG breakage when the attached OFS on a CFRP-reinforced concrete beam ruptured under continuous compressive loading. The first FBG failed when the load reached 314.5 kN, while another failed above 900 kN. The authors credited the fiber breakage to the load eccentricity or non-uniform load distribution on the composite structure.

Additionally, previous literature reported that FBG breaks beyond a certain strain or stress value. Therefore, it could be argued that sensor failure after exceeding a certain load or stress threshold is an excellent criterion to consider its suitability with the intended application. Certain applications might require a higher parameter sensing value, which might not be suitable for FBG due to its possible failure. This, in turn, depends on the material properties of the manufactured optical fiber, especially the typical mechanical properties of FBG materials, as listed in Table 5. Therefore, it is crucial to ensure that the host composite’s mechanical properties and intended service load do not exceed those of FBG.

TABLE 5. Typical mechanical properties of FBG from past studies [68], [139], [140], [141].

Material type	Young’s modulus, E (GPa)	Shear modulus, G (GPa)	Poisson’s ratio, ν
Silica glass	70.00–72.90	31.10	0.17–0.33

D. CROSS-SENSITIVITY OF FBG

It is well-known that FBG is highly-responsive to strain and temperature perturbations [55]. This consequently raises an ongoing issue of separating the FBG wavelength shift between strain and temperature, especially in applications requiring one to conduct mono-parameter sensing with the influence of other parameters. Over the past decades, the most common method to cater to this was to employ two FBGs, with one of the FBG encapsulated inside a capillary tubing prior to being embedded inside or attached to the surface of the composite laminates [78], [88], [127]. As the encapsulated FBG is always in a strain-free state, the different readings with the bare FBG can differentiate between the actual temperature and the true strain perturbation shift from the FBG spectra. As has been covered in earlier sub-sections, this method was thought to cause microstructural disturbance to the local vicinity of the host composite, consequently affecting its mechanical properties. Adding to this was the fact that one must include a separate FBG sensor for each parameter for sensing purposes, which could be costly and involve a more complex sensing system. Not to mention

that embedding multiple FBGs, especially with encapsulation tubes, might exacerbate the local microstructural perturbation effect.

In the past, numerous researchers have continuously explored alternative options to enable multiparameter sensing, possibly without the need to perform temperature-compensated strain measurement using capillary tubes, as reported before. To avoid using multiple OFS, Kang et al. [80] used FBG in tandem with EFPI as a sensor. However, both optical fibers were still enclosed inside a capillary tube. Rao et al. [104] adopted a similar approach to Kang et al. [80], but the encapsulated optical fibers were surface-mounted on the composite. Meanwhile, Yoon et al. [81] spliced two FBG gratings made from glass of different dopant concentrations so that the only sensitivity towards strain is identical, but not temperature. Furthermore, Rocha et al. [88] used smaller FBGs with a smaller encapsulated tube to mitigate the effect of microstructural perturbation, while Oromiehe et al. [89] embedded two FBGs, with one implanted at a slightly different angle so that the slightly different strain caused may cater for the cross-sensitivity issue. Keulen et al. [2] multiplexed FBG with EFS to monitor flow and strain so that different OFS will monitor different parameters. Nevertheless, these methods showed promising potential to cater to the cross-sensitivity issue of FBG. Continuous efforts are currently in progress to address this ongoing and unsolved issue.

E. SPATIAL COVERAGE OF FBG SENSORS

Despite the numerous advantages of FBG, one of its drawbacks is its limited sensing vicinity. Although it is generally known that FBG is highly sensitive to external perturbations, such as temperature change or strain, this high sensitivity might have limited its sensing capabilities to only point sensing. There are a few available methods that cater to this issue. Among them is by adopting distributed or quasi-distributed FBG sensing, which usually involves inscribing Bragg gratings on numerous equidistant points on an optical fiber. This method is called multiplexing; it can be done by time, space, wavelength division multiplexing, or any combination. Regardless, multiplexing might have just increased the complexity of the sensing system, as additional sensing components are usually needed to cater to the increase in sensing power, such as a demodulator, which will not be cost-effective. Not to mention that multiplexing FBG also suffer from sampling frequency problem, as not many technologies currently support the high-speed frequency of multiplexed FBG, as claimed by previous studies [113], [114]. While multiplexed FBG might be able to conduct distributed or quasi-distributed sensing, the sensing accuracy might have been compromised. Zhu et al. [142] claimed a significant optical power loss on the last sensor position of a 10-multiplexed FBG sensor system due to the accrued optical power loss from the preceding sensor as a result of induced micro-bending optical loss.

F. SENSOR LOCATION AND PLACEMENT

For both embedded and surface-mounted FBGs, its location of placement plays a vital role and is highly related to the sensing capabilities of the optical fiber. Certain applications require the FBG to be perfectly placed at specific locations, or the sensor will not function efficiently. Several past studies opted for numerical and analytical simulations to determine the optimal embedding or the FBG placement location [133], [143], [144] and have shown deteriorated sensing capabilities when placed other than at the optimal location. Apart from the placement location, the orientation of FBG has also been proven to impact its sensing capabilities directly. A study by Basu and Ghorai [65] demonstrated that FBG sensors orientated increasingly transversal to the direction of the reinforcing fiber reduced the sensing capabilities by nearly 90%. Similarly, Shivakumar and Emmanwori [138] witnessed a drop in the mechanical properties of the host composite by up to 40% and 15% for 8-ply and 16-ply composite laminates, respectively. On the other hand, Sonnenfield et al. [128] observed fluctuation in the sensing capabilities of its anisotropic geometrically-birefringent FBG as it ‘rotated’ about its fiber axis, causing the perturbation sensed not efficiently to transfer to the sensor grating.

In addition to these critical issues, FBG embedment inside composite laminates presents another problem: the optical fiber’s ingress and egress location are the weakest and most vulnerable to failure, especially during the in-mold manufacturing, such as VARIM, VARTM, hot-press, or vacuum-bagging. Most researchers adopted capillary tubing made from high-resilience materials, such as rubber or Teflon, to encase the optical fibers at the ingress and egress locations to protect them from additional load and prevent fiber breakage [122], [129]. However, the protruding encased optical fiber might act as a stress concentrator and assist in fiber debonding or delamination, which hastens the composite laminate failure. Another alternative solution is to adopt detachable connectors. Previously, Basile et al. [131] proposed the use of detachable magnetic connectors, while Tsutsui et al. [132] demonstrated the use of embedded connectors for smart composite in an aircraft structural damage detection system. Besides that, embedding multiple FBG sensors in between multiple layers –as conducted by Chen et al. [62] to study the curing temperature through the thickness of the composite laminate – might be detrimental to the mechanical properties of the host composite. As discussed in Sub-Sections IX-A and IX-B, improper FBG embedment might disturb the microstructural integrity in the vicinity of the FBG itself. Therefore, it is not advisable to incorporate multiple FBG sensors onto different layers of the lamina in a real-world application manufacturing process.

G. FBG AS SENSORS FOR ADVANCED COMPOSITES

As extensively shown throughout this paper, FBG is a highly-capable multiparameter sensor to be employed on or inside FRP composite laminates. With FRPs being a high-end material sought after by various high-end industrial

applications, this has undoubtedly put FBG into the interest of researchers and industrialists to be utilized as valuable sensors. Nevertheless, it is intriguing to investigate if FBG can be further manipulated as a sensing system for other composite materials, such as polymeric foam, honeycomb core, or corrugated core. It is worth pointing out that the three types of composites mentioned above are commonly paired with FRP laminates in a ‘sandwich composites’ system, which is made up of one low-density composite core sandwiched between two highly-stiff composite laminates. Therefore, it is interesting to determine if the FBG sensing system already existing in FRPs could be further extended as a sensor for sandwich cores in a sandwich composite system in real-world applications. The challenge would be properly placing the OFS, as the composite cores comprise unusual and irregular shapes and surfaces, as demonstrated in Figure 29. An early attempt to integrate optical fiber sensing for sandwich composites was performed by Kulpa et al. [145], who utilized a distributed optical fiber sensing system as strain and displacement sensors embedded in polyurethane foam-filled honeycomb-ribbed core sandwich composites.

X. FUTURE PROSPECT OF FBG AS SENSORS

Based on past literature, the previous sub-sections have thoroughly reviewed the usage of FBG as multiparameter sensors in fiber-reinforced composite laminates under various conditions, providing mixed normal and peculiar experimental feedback. This was followed by an in-depth discussion on several outstanding issues affiliated with FBG sensors, particularly its application in polymer composite laminates. It is clear from this paper that research regarding the application of FBG in composite material sensing will continue to flourish and evolve.

It is highly suggestive that all previous efforts were made to achieve a common target, which is to enhance the reliability and accuracy of FBG sensing. Numerous methods have been explored and employed in the past, including Finite Element Method (FEM) optimization, optimal sensor placement, FBG coating manipulation, FBG orientation manipulation, and addressing cross-sensitivity issues [6], [96], [97], [127]. The methods mentioned above have been verified to enhance FBG reliability and accuracy to a certain degree. However, as the global community is now embracing the transition towards Industrial Revolution 4.0 (IR4.0), a shift in trend in FBG accuracy-enhancement methods is apparent, leaning more towards utilization of computerized software, which includes optimization, algorithms, NN, and Deep Learning (DL). They involve complex mathematical modeling and solving, pattern and trend recognition, and an even more complex decision-making process; based on some preliminary experimental data used as input. A summary of work utilizing these kinds of methods is shown in Table 6.

In tandem with the emergence of IR4.0 and the transition to less experimental-based research and more simulation-based studies, there is also a demand for functional, more compact, energy-efficient, and low-cost machinery. This implies the

TABLE 6. Details on selected works utilizing NN, algorithms, or DL to improve FBG sensing.

Experimental details/Application	Parameter	ML type	Ref.
FBG as temperature/strain sensors in CFRP	Strain, temperature	Multilayer perceptron NN	[93]
FBG for SHM in aircraft composite wing structure	Strain	Algorithm	[15]
FBG as SHM of composite-stiffened panel in aircraft structure to detect damage	Dynamic strain	Algorithm, Artificial Neural Network (ANN)	[108]
Embedded FBG as damage detection mechanism via 'coordinate'	Strain, damage	NN	[113,114]
FBG as an MRI-compatible tactile sensor in the medical field	Strain	Backpropagation NN	[159]
FBG as a sensor system for impact localization of aircraft composite wing structure	Strain	Localization algorithm	[109]
FBG as a three-axis force sensor in robot-surgery application	Strain	Two-layer feed-forward NN	[160]
Impact damage and localization using FBG	Strain, damage	Optimization	[161]
FBG as strain sensor in wearable hand device to track hand movement	Strain	Algorithm	[40]

necessity for a more compact and portable sensing system, which in the case of this present paper, is the application of FBG. It is not an overstatement for a complete sensing system using FBG, even for a single parameter made up of complex equipment and not to mention space-consuming. While the space or size of the equipment is of concern, it is essential to highlight that any reduction in the size of the equipment should never jeopardize the reliability or accuracy of the sensing system itself, which is a challenge to be addressed during the implementation of IR4.0. Mizutani et al. [120] have attempted to address this issue in which they had to

manufacture a novel lightweight and smaller FBG demodulator to fit the weight limit of the reusable rocket to which it was intended to be applied to. This work could spearhead more research into developing a more portable high-end FBG sensing system.

In an effort to further enhance the sensing competence of FBG, it is highly indicative that hybridized FBG sensors will take the spotlight soon. By splicing or connecting different OFSSs using adhesive, different responses on different perturbations can be obtained, leading to more efficient multiparameter sensing. Moreover, this method also seems to address the cross-sensitivity issue of the FBG, which is a major drawback and has undoubtedly limited the application of FBG as sensors. Numerous works have demonstrated the feasibility of hybridizing FBG using several types of OFSSs, including EFPI [64], [80], [104], long-period grating (LPG) [32], [146], and Mach-Zehnder interferometer (MZI) [147], [148]. With the flourishing and continuous efforts by researchers and industrialists to improve the competency of FBG, it is highly feasible to anticipate more unorthodox hybridization of FBG with other types of OFSSs in the future.

Recent breakthroughs in FBG measurement techniques could also lead to a significant improvement in FRP monitoring. Recently, a new concept of distributed sensing based on large-scale FBG arrays has been introduced with high spatial resolution (< 10 mm), small grating spacing (1 mm), and large multiplexing capacity up to a few thousand sensor units [149]. This technique provides high resolution measurement, allowing 2D or 3D strain or temperature mapping at the targeting area [150], [151] which could enhance the quality of FRP composite monitoring. The reflection spectrum of the FBG could also provide a very localized strain distribution across the FBG. Several strain distribution reconstruction techniques have been proposed to address the non-uniform strain distribution impacted along the FBG length [152], [153], [154] which could provide a vital explanation for the complex failure mechanism of FRP composites. The capability of FBG sensors as 3D shape sensors realized using multicore fiber [155] could also be implemented in certain FRP composite monitoring applications that require knowledge about the direction of curvature and twisting of the FRP composites. All of these additional capabilities offer innovative solutions to a variety of engineering issues and should be rapidly translated into user-accessible commercial products.

In the current market, the customized multiplexed FBG sensors are sold at high price. As the demand for FBG sensors rises and FBG sensors become a standard instrument, it is imperative that FBG writing equipment become accessible to researchers at a low cost. Possessing a FBG writing system would allow researchers to tailor FBG designs and implement FBG sensor networks without any constraints. The common writing techniques adopted by commercial systems are based on direct writing [156], interferometric and phase mask techniques [157], with most development focusing on the enhancement of automation and software control, multiple sensors writing capability, positional accuracy, and

reproducibility of center wavelength. It has been demonstrated previously that by combining the fiber drawing process with the grating writing process, the manufacturing time of large scale FBG sensor networks can be dramatically reduced [158]. Based on the ongoing trend, the cost of the FBG writing system will gradually decrease in the future while providing ever-more advanced capabilities. FBG sensors are expected to become increasingly important in the monitoring of FRP composites and other engineering applications as a result of their great sensing capabilities, which cannot be replicated by other techniques.

XI. SUMMARY

This paper has provided a comprehensive review regarding the application of FBG as either a single or multiparameter sensor in fiber-reinforced polymer composite laminates. The background of FBG was first presented, including the application of FBGs other than in composite laminates and the working principle behind FBG. Following this, a detailed and elaborate literature review was provided, essentially dividing the topic into two major themes, mainly embedded and surface-mounted FBG. The ideal guidelines for FBG embedding procedures and techniques were also discussed, which will benefit future researchers and industrialists. Furthermore, relevant issues were highlighted and discussed, with the paper ending with a projected overview of how FBG will evolve and fare in the upcoming years.

Regardless of whether embedded or surface-mounted, FBG has shown an unambiguous competency as a strain and temperature sensor. Moreover, it has demonstrated the ability as damage detection, impact source triangulation, pressure, and flow sensor. It is also evident from past literature that only marginal difference exists in terms of the measured parameter sensitivity between both types of FBG deployment methods. Apart from selecting the embedded or surface-attached approach, the location of FBG on the laminate has proven to be a pivotal factor in determining the efficiency of the optical fiber laminates. Hence, obtaining the optimal location often requires either preliminary tests or optimization via finite element analysis.

Regarding optimization, it is highly indicative that most FBG sensing applications will be paired with optimization components in the foreseeable future, such as ANN, algorithms, Machine Learning (ML), and Artificial Intelligence (AI), especially with IR4.0 currently in motion. It is also intriguing to anticipate the application of FBG as a sensor in other composite materials, such as polymeric or metallic foam composites, honeycomb cores, corrugated foam, and sandwich structures. Continuous efforts by researchers and industrialists are

REFERENCES

- [1] O. Ahmed, X. Wang, M. V. Tran, and M. Z. Ismadi, "Advancements in fiber-reinforced polymer composite materials damage detection methods: Towards achieving energy-efficient SHM systems," *Compos. B. Eng.*, vol. 223, pp. 1–23, Oct. 2021, doi: 10.1016/j.compositesb.2021.109136.
- [2] C. J. Keulen, M. Yildiz, and A. Suleman, "Multiplexed FBG and etched fiber sensors for process and health monitoring of 2- & 3-D RTM components," *J. Reinforced Plastics Compos.*, vol. 30, no. 12, pp. 1055–1064, Aug. 2011, doi: 10.1177/0731684411411960.
- [3] C. A. Chairman and S. P. K. Babu, "Mechanical and abrasive wear behavior of glass and basalt fabric-reinforced epoxy composites," *J. Appl. Polym. Sci.*, vol. 130, no. 1, pp. 120–130, Mar. 2013, doi: 10.1002/app.39154.
- [4] P. Luangtriratana, B. K. Kandola, and P. Myler, "Ceramic particulate thermal barrier surface coatings for glass fibre-reinforced epoxy composites," *Mater. Des.*, vol. 68, pp. 232–244, Mar. 2015, doi: 10.1016/j.matdes.2014.11.057.
- [5] G. Wu, X. Wang, Z. Wu, Z. Dong, and G. Zhang, "Durability of basalt fibers and composites in corrosive environments," *J. Compos. Mater.*, vol. 49, no. 7, pp. 873–887, Mar. 2014, doi: 10.1177/0021998314526628.
- [6] J. Wang, Z. Wang, Q. Sui, L. Jia, Y. Li, M. Han, X. Wang, and H. Lin, "Development of smart CFRP composites embedded with FBG sensors," in *Proc. Chin. Autom. Congr. (CAC)*, Oct. 2017, pp. 2593–2597, doi: 10.1109/CAC.2017.8243213.
- [7] D. Kinet, P. Mégret, K. Goossen, L. Qiu, D. Heider, and C. Caucheteur, "Fiber Bragg grating sensors toward structural health monitoring in composite materials: Challenges and solutions," *Sensors*, vol. 14, no. 4, pp. 7394–7419, Apr. 2014, doi: 10.3390/s140407394.
- [8] L. Fan, and Y. Bao, "Review of fiber optic sensors for corrosion monitoring in reinforced concrete," *Cement Concrete Compos.*, vol. 120, pp. 1–19, Jul. 2012, doi: 10.1016/j.cemconcomp.2021.104029.
- [9] Y. Dong, "Non-destructive evaluation (NDE) of polymer matrix composites," in *Non-Destructive Evaluation (NDE) of Composites: Using Fiber Optic Sensor*. Amsterdam, The Netherlands: Elsevier, 2013, ch. 23, pp. 617–633.
- [10] Y. Weng, X. Qiao, T. Guo, M. Hu, Z. Feng, R. Wang, and J. Zhang, "A robust and compact fiber Bragg grating vibration sensor for seismic measurement," *IEEE Sensors J.*, vol. 12, no. 4, pp. 800–804, Apr. 2012, doi: 10.1109/JSEN.2011.2166258.
- [11] A. Bagchi, E. Murison, A. A. Mufti, and A. S. Noman, "Evaluation of a rugged FBG strain sensor system for monitoring reinforced concrete structures," *Exp. Techn.*, vol. 34, no. 2, pp. 49–53, Mar. 2010, doi: 10.1111/j.1747-1567.2009.00526.x.
- [12] E. Oromicchie, B. G. Prusty, G. Rajan, and P. Compston, "Optical fiber Bragg grating sensors for process monitoring in advanced composites," in *Proc. IEEE Sensors Appl. Symp. (SAS)*, Apr. 2016, pp. 1–5, doi: 10.1109/SAS.2016.7479849.
- [13] A. Annunziato, F. Anelli, J. Gates, C. Holmes, and F. Prudenano, "Design of polarization-maintaining FBGs using polyimide films to improve strain-temperature sensing in CFRP laminates," *IEEE Photon. J.*, vol. 13, no. 2, pp. 1–15, Apr. 2021, doi: 10.1109/JPHOT.2021.3063172.
- [14] G. C. Kahandawa, J. Epaarachchi, H. Wang, and K. T. Lau, "Use of FBG sensors for SHM in aerospace structures," *Photon. Sens.*, vol. 2, pp. 203–214, Jun. 2021, doi: 10.1007/s13320-012-0065-4.
- [15] B. Moslehi, R. J. Black, and F. Faridian, "Multifunctional fiber Bragg grating sensing system for load monitoring of composite wings," in *Proc. Aerosp. Conf.*, Mar. 2011, pp. 1–9, doi: 10.1109/AERO.2011.5747387.
- [16] H. Cao, Y. Hao, Z. Zhang, J. Wei, and L. Yang, "System and method of quasi-distributed fiber Bragg gratings monitoring brittle fracture process of composite insulators," *IEEE Trans. Instrum. Meas.*, vol. 70, pp. 1–10, 2021, doi: 10.1109/TIM.2021.3096876.
- [17] W. Xiao-Dong, N. Jing, X. Tao, and L. Yao-Qin, "On-line monitoring technology of UHV composite insulator based on FBG sensor," in *Proc. IEEE Sustain. Power Energy Conf. (iSPEC)*, Nov. 2019, pp. 2901–2904, doi: 10.1109/iSPEC48194.2019.8974937.
- [18] Y. Qiu, Q.-B. Wang, H.-T. Zhao, J.-A. Chen, and Y.-Y. Wang, "Review on composite structural health monitoring based on fiber Bragg grating sensing principle," *J. Shanghai Jiaotong Univ. Sci.*, vol. 18, no. 2, pp. 129–139, Apr. 2013, doi: 10.1007/s12204-013-1375-4.
- [19] K.-T. Lau, "Structural health monitoring for smart composites using embedded FBG sensor technology," *Mater. Sci. Technol.*, vol. 30, no. 13, pp. 1642–1654, Jul. 2014, doi: 10.1179/1743284714Y.0000000608.
- [20] G. Luyckx, E. Voet, N. Lammens, and J. Degrieck, "Strain measurements of composite laminates with embedded fibre Bragg gratings: Criticism and opportunities for research," *Sensors*, vol. 11, no. 1, pp. 384–408, Dec. 2010, doi: 10.3390/s110100384.

- [21] N. Takeda and Y. Okabe. "Fiber Bragg grating sensors: Recent advancements, industrial applications and market exploitation," in *Fiber Bragg Grating Sensors in Aeronautics and Astronautics*. Bentham Science Publishers, 2011, ch. 14, pp. 171–184.
- [22] D. Tosi, M. Olivero, G. Perrone, A. Vallan, and L. Arcudi. "Simple fiber Bragg grating sensing systems for structural health monitoring," in *Proc. IEEE Workshop Environ., Energy, Struct. Monitor. Syst.*, Sep. 2009, pp. 80–86, doi: 10.1109/EESMS.2009.5341310.
- [23] A. G. Leal-Junior and C. Marques. "Diaphragm-embedded optical fiber sensors: A review and tutorial," *IEEE Sensors J.*, vol. 21, no. 11, pp. 12719–12733, Jun. 2021, doi: 10.1109/JSEN.2020.3040987.
- [24] C. Marques, A. Leal-Junior, and S. Kumar. "Multifunctional integration of optical fibers and nanomaterials for aircraft systems," *Materials*, vol. 16, no. 4, pp. 1–29, Feb. 2023, doi: 10.3390/ma16041433.
- [25] K. O. Hill, Y. Fujii, D. C. Johnson, and B. S. Kawasaki. "Photosensitivity in optical fiber waveguides: Application to reflection filter fabrication," *Appl. Phys. Lett.*, vol. 32, no. 10, pp. 647–649, Aug. 2008, doi: 10.1063/1.89881.
- [26] D. K. W. Lam and B. K. Garside. "Characterization of single-mode optical fiber filters," *Appl. Opt.*, vol. 20, no. 3, pp. 440–445, Feb. 1981, doi: 10.1364/AO.20.000440.
- [27] G. Meltz, W. W. Morey, and W. H. Glenn. "Formation of Bragg gratings in optical fibers by a transverse holographic method," *Opt. Lett.*, vol. 14, no. 15, pp. 823–825, 1989, doi: 10.1364/OL.14.000823.
- [28] W. Morey, G. Meltz, and H. Glenn. "Fiber optic Bragg grating sensors," *Proc. SPIE*, vol. 1169, pp. 98–107, Feb. 1990, doi: 10.1117/12.963022.
- [29] S. M. Melle, A. T. Alavie, S. Karr, T. Coroy, K. Liu, and R. M. Measures. "A Bragg grating-tuned fiber laser strain sensor system," *IEEE Photon. Technol. Lett.*, vol. 5, no. 2, pp. 263–266, Feb. 1993, doi: 10.1109/68.196025.
- [30] A. D. Kersey and T. A. Berkoff. "Fiber-optic Bragg-grating differential-temperature sensor," *IEEE Photon. Technol. Lett.*, vol. 4, no. 10, pp. 3–5, Oct. 1992, doi: 10.1109/68.163773.
- [31] A. D. Kersey and W. W. Morey. "Multiplexed Bragg grating fibre-laser strain-sensor system with mode-locked interrogation," *Electron. Lett.*, vol. 29, no. 1, pp. 112–114, Jan. 1993, doi: 10.1049/el:19930073.
- [32] B. Yang, X. Tao, and J. Yu. "Fibre Bragg grating sensor for simultaneous measurement of strain and temperature," *J. Ind. Textiles*, vol. 34, no. 2, pp. 97–115, Oct. 2004, doi: 10.1177/1528083704046609.
- [33] L. Ren, G. Song, M. Condit, P. C. Noble, and H. Li. "Fiber Bragg grating displacement sensor for movement measurement of tendons and ligaments," *Appl. Opt.*, vol. 46, no. 28, pp. 6867–6871, 2007, doi: 10.1364/AO.46.006867.
- [34] L. Li, R. He, M. S. Soares, S. Savovic, X. Hu, C. Marques, R. Min, and X. Li. "Embedded FBG-based sensor for joint movement monitoring," *IEEE Sensors J.*, vol. 21, no. 23, pp. 26793–26798, Dec. 2021, doi: 10.1109/JSEN.2021.3120995.
- [35] M. Vilimek. "Using a fiber Bragg grating sensor for tendon force measurements," *J. Biomech.*, vol. 41, no. 1, p. S511, Jul. 2008, doi: 10.1016/S0021-9290(08)70510-4.
- [36] M. I. Zibani, H. Latifi, F. Karami, A. Ronaghi, S. C. Nejad, and L. Dargahi. "In vivo brain temperature measurements based on fiber optic Bragg grating," in *Proc. 25th Opt. Fiber Sensors Conf. (OFS)*, Apr. 2017, Art. no. 103234G, doi: 10.1117/12.2265607.
- [37] A. Kalinowski, L. Z. Karam, V. Pegorini, A. B. Di Renzo, C. S. R. Pitta, R. Cardoso, T. S. Assmann, H. J. Kalinowski, and J. C. C. da Silva. "Optical fiber Bragg grating strain sensor for bone stress analysis in bovine during masticatory movements," *IEEE Sensors J.*, vol. 17, no. 8, pp. 2385–2392, Apr. 2017, doi: 10.1109/jсен.2017.2667618.
- [38] K. Ogawa, S. Koyama, H. Ishizawa, S. Fujiwara, and K. Fujimoto. "Simultaneous measurement of heart sound, pulse wave and respiration with single fiber Bragg grating sensor," in *Proc. IEEE Int. Symp. Med. Meas. Appl. (MeMeA)*, Jun. 2018, pp. 1–5, doi: 10.1109/MeMeA.2018.8438629.
- [39] S. Pant, S. Umesh, and S. Asokan. "Fiber Bragg grating respiratory measurement device," in *Proc. IEEE Int. Symp. Med. Meas. Appl. (MeMeA)*, Jun. 2018, pp. 1–5, doi: 10.1109/MeMeA.2018.8438774.
- [40] J. J. S. Kim, B. K. Kim, M. Jang, B.-K. K. Ju, J. J. S. Kim, K. Kang, D. E. Kim, B. K. K. Ju, and J. J. S. Kim. "Wearable hand module and real-time tracking algorithms for measuring finger joint angles of different hand sizes with high accuracy using FBG strain sensor," *Sensors*, vol. 20, no. 7, pp. 1–20, Mar. 2020, doi: 10.3390/s20071921.
- [41] D. Shin and T. Kim. "Wearable sensor based on fiber Bragg grating with flexible polymer for squat exercise," in *Proc. IEEE Int. Workshop Metrol. Ind. IoT (MetroInd&IoT)*, Jun. 2021, pp. 478–481, doi: 10.1109/MetroInd4.0IoT51437.2021.9488544.
- [42] N. V. Kumar, S. Pant, S. Sridhar, V. Marulasiddappa, S. Srivatsen, and S. Asokan. "Fiber Bragg grating-based pulse monitoring device for real-time non-invasive blood pressure measurement—A feasibility study," *IEEE Sensors J.*, vol. 21, no. 7, pp. 9179–9185, Apr. 2021, doi: 10.1109/JSEN.2021.3055245.
- [43] V. V. Spirin, M. G. Shlyagin, S. V. Miridonov, F. J. M. Jiménez, and R. M. L. Gutiérrez. "Fiber Bragg grating sensor for petroleum hydrocarbon leak detection," *Opt. Lasers Eng.*, vol. 32, no. 5, pp. 497–503, Nov. 1999, doi: 10.1016/S0143-8166(00)00021-X.
- [44] Z. Y. Zhong, X. L. Zhi, and W. J. Yi. "Oil well real-time monitoring with downhole permanent FBG sensor network," in *Proc. IEEE Int. Conf. Control Autom.*, Jun. 2007, pp. 2591–2594, doi: 10.1109/ICCA.2007.4376830.
- [45] R. C. Kamikawachi, I. Abe, H. J. Kalinowski, J. L. Fabris, and J. L. Pinto. "Thermal characterization of etched FBG for applications in oil and gas sector," in *Proc. SBMO/IEEE MIT-S Int. Microw. Optoelectron. Conf.*, Nov. 2007, pp. 280–283, doi: 10.1109/IMOC.2007.4404263.
- [46] A. Samavati, M. Velashjerdi, A. F. Ismail, M. H. D. Othman, G. B. Eisaabadi, A. Awang, Z. Samavati, A. Rostami, and N. Yahya. "Continuous monitoring of crude oil movement in an electromagnetic-assisted enhanced oil recovery process using a modified fiber Bragg grating sensor," *Sens. Actuators A, Phys.*, vol. 318, pp. 1–12, Feb. 2021, doi: 10.1016/j.sna.2020.112428.
- [47] J. Johny, R. Prabhu, W. K. Fung, and J. Watson. "Investigation of positioning of FBG sensors for smart monitoring of oil and gas subsea structures," in *Proc. OCEANS*, Apr. 2016, pp. 1–4, doi: 10.1109/OCEANSAP.2016.7485662.
- [48] G. B. Tait, G. C. Tepper, D. Pestov, and P. M. Boland. "Fiber Bragg grating multi-functional chemical sensor," *Proc. SPIE*, vol. 5994, Nov. 2005, Art. no. 599407, doi: 10.1117/12.628394.
- [49] P. Boland, G. Sethuraman, A. Mendez, T. Graver, D. Pestov, and G. Tait. "Fiber Bragg grating multichannel sensor," *Proc. SPIE*, vol. 6371, Oct. 2006, Art. no. 637109, doi: 10.1117/12.686056.
- [50] G. Lyu, Z. Song, X. Jiang, L. Wang, G. Che, and X. Shen. "A novel fibre grating gas flow sensor," *Pacific Sci. Rev.*, vol. 16, no. 1, pp. 19–22, Jun. 2014, doi: 10.1016/j.pscr.2014.08.003.
- [51] S. M. A. Musa, R. R. Ibrahim, and A. I. Azmi. "Development of fiber Bragg grating (FBG) as temperature sensor inside packed-bed non-thermal plasma reactor," *Jurnal Teknologi*, vol. 68, no. 3, pp. 139–142, May 2014, doi: 10.11113/jt.v68.2960.
- [52] J. Jiang, G.-M. Ma, C.-R. Li, H.-T. Song, Y.-T. Luo, and H.-B. Wang. "Highly sensitive dissolved hydrogen sensor based on side-polished fiber Bragg grating," *IEEE Photon. Technol. Lett.*, vol. 27, no. 13, pp. 1453–1456, Jul. 1, 2015, doi: 10.1109/LPT.2015.2425894.
- [53] S. J. Spammera and P. L. Fuhr. "Concrete embedded optical fibre Bragg grating strain sensors," in *Proc. IEEE ISIE*, Jul. 1998, pp. 330–334, doi: 10.1109/ISIE.1998.707802.
- [54] Y. Zhou and Y. F. Wang. "Creep monitoring for subway station structure by fiber Bragg grating sensors," in *Proc. Int. Conf. Optoelectron. Image Process.*, Nov. 2010, pp. 358–361, doi: 10.1109/ICOIP.2010.21.
- [55] M. R. Mokhtar, K. Owens, J. Kwasny, S. E. Taylor, P. A. M. Basheer, D. Cleland, Y. Bai, M. Sonebi, G. Davis, A. Gupta, I. Hogg, B. Bell, W. Doherty, S. McKeague, D. Moore, K. Greeves, T. Sun, and K. T. V. Grattan. "Fiber-optic strain sensor system with temperature compensation for arch bridge condition monitoring," *IEEE Sensors J.*, vol. 12, no. 5, pp. 1470–1476, May 2012, doi: 10.1109/JSEN.2011.2172991.
- [56] G. Rajan, S. Jinachandran, J. Xi, H. Li, J. S. Vinod, T. Moses, S. Karekal, and B. G. Prusty. "Fibre optic acoustic emission measurement technique for crack activity monitoring in civil engineering applications," in *Proc. SAS*, 2016, pp. 232–235, doi: 10.1109/SAS.2016.7479851.
- [57] R. Min, Z. Liu, L. Pereira, C. Yang, Q. Sui, and C. Marques. "Optical fiber sensing for marine environment and marine structural health monitoring: A review," *Opt. Laser Technol.*, vol. 140, pp. 1–12, Mar. 2021, doi: 10.1016/j.optlastec.2021.107082.
- [58] T. Liao, Y. Pei, J. Xu, H. Lin, and T. Ning. "Fiber Bragg grating temperature sensors applied in harsh environment of aerospace," in *Proc. Asia Commun. Photon. Conf. (ACP)*, Oct. 2018, pp. 1–3, doi: 10.1109/ACP.2018.8595842.

- [59] Y. Pei, T. Liao, Y. Pei, J. Xu, H. Lin, and T. Ning, "FBG strain sensor applied in harsh environment of aerospace," in *Proc. IEEE 3rd Optoelectron. Global Conf. (OGC)*, Sep. 2018, pp. 81–84, doi: 10.1109/OGC.2018.8529994.
- [60] P. D. Foote, "Optical fibre Bragg grating sensors for aerospace smart structures," in *Proc. IEE Colloq. Opt. Fibre Grating Their Appl.*, 1995, pp. 14-1–14-6, doi: 10.1049/ic:19950093.
- [61] X. Yang, M. Li, D. Wei, and X. Kou, "Application of large strain fiber grating sensing technology in aircraft structural health monitoring," in *Proc. IEEE Int. Conf. Inf. Technol., Big Data Artif. Intell. (ICIBA)*, Nov. 2020, pp. 23–27, doi: 10.1109/ICIBA50161.2020.9277124.
- [62] J. Chen, J. Wang, X. Li, L. Sun, S. Li, and A. Ding, "Monitoring of temperature and cure-induced strain gradient in laminated composite plate with FBG sensors," *Compos. Struct.*, vol. 242, pp. 1–9, Mar. 2020, doi: 10.1016/j.compstruct.2020.112168.
- [63] M. Harsch, J. Karger-Kocsis, and F. Herzog, "Influence of cure regime on the strain development in an epoxy resin as monitored by a fiber Bragg grating sensor," *Macromolecular Mater. Eng.*, vol. 292, no. 4, pp. 474–483, Apr. 2007, doi: 10.1002/mame.200600432.
- [64] T. Kosaka, H. Kurimoto, K. Osaka, A. Nakai, T. Osada, H. Hamada, and T. Fukuda, "Strain monitoring of braided composites by using embedded fiber-optic strain sensors," *Adv. Compos. Mater.*, vol. 13, nos. 3–4, pp. 157–170, Jan. 2004, doi: 10.1163/1568551042580172.
- [65] M. Basu and S. K. Ghorai, "Strain sensing in fiber-reinforced polymer laminates using embedded fiber Bragg grating sensor," *Fiber Integr. Opt.*, vol. 33, no. 4, pp. 279–298, Aug. 2014, doi: 10.1080/01468030.2014.906686.
- [66] X. Shen and Y. Lin, "Measurements of temperature and residual strain during fatigue of a CFRP composite using FBG sensors," in *Proc. Int. Conf. Measuring Technol. Mechatron. Autom. (ICMTMA)*, Apr. 2009, pp. 35–38, doi: 10.1109/ICMTMA.2009.336.
- [67] G. Luyckx, F. Voet, T. Geernaert, K. Chah, T. Nasilowski, W. De Waele, W. Van Paeppegem, M. Becker, H. Bartelt, W. Urbanczyk, J. Wojcik, J. Degrieck, F. Berghmans, and H. Thienpont, "Response of FBGs in microstructured and how the fibers embedded in laminated composite," *IEEE Photon. Technol. Lett.*, vol. 21, no. 18, pp. 1290–1292, Sep. 2009, doi: 10.1109/LPT.2009.2025262.
- [68] A. Papanthiou, G. Rigas, and N. D. Alexopoulos, "Assessment of the strain monitoring reliability of fiber Bragg grating sensor (FBGs) in advanced composite structures," *Compos. Struct.*, vol. 93, no. 9, pp. 2163–2172, Aug. 2011, doi: 10.1016/j.compstruct.2011.03.001.
- [69] S. Sulejmani, C. Sonnenfeld, T. Geernaert, F. Berghmans, H. Thienpont, S. Fve, N. Lammens, G. Luyckx, F. Voet, J. Degrieck, W. Urbanczyk, P. Mergo, M. Becker, and H. Bartelt, "Towards micro-structured optical fiber sensors for transverse strain sensing in smart composite materials," in *Proc. IEEE SENSORS*, Oct. 2011, pp. 109–112, doi: 10.1109/ICSENS.2011.6127305.
- [70] F. Braghin, G. Cazzulani, S. Cinquemani, and F. Resta, "Potential of FBG sensors for vibration control in smart structures," in *Proc. IEEE Int. Conf. Mechatronics (ICM)*, Feb. 2013, pp. 186–191, doi: 10.1109/ICMECH.2013.6518533.
- [71] G. Rajan, M. Ramakrishnan, Y. Semenova, E. Ambikairajah, G. Farrell, and G.-D. Peng, "Experimental study and analysis of a polymer fiber Bragg grating embedded in a composite material," *J. Lightw. Technol.*, vol. 32, no. 9, pp. 1726–1733, May 2014, doi: 10.1109/JLT.2014.2311441.
- [72] U. Sampath, D.-G. Kim, H. Kim, and M. Song, "Fiber-optic sensor for simultaneous strain and temperature monitoring in composite materials at cryogenic condition," in *Proc. 25th Opt. Fiber Sensors Conf. (OFS)*, Apr. 2017, Art. no. 1032347, doi: 10.1117/12.2265533.
- [73] Q. Zhu, C. Xu, and G. Yang, "Experimental research on damage detecting in composite materials with FBG sensors under low frequency cycling," *Int. J. Fatigue*, vol. 101, no. 1, pp. 61–66, Aug. 2017, doi: 10.1016/j.ijfatigue.2017.03.034.
- [74] W. Chen and M. Tang, "Monitoring on internal temperature of composite insulator with embedding fiber Bragg grating for early diagnosis," in *Proc. 25th Opt. Fiber Sensors Conf. (OFS)*, Apr. 2017, Art. no. 103236X, doi: 10.1117/12.2264374.
- [75] K. Bremer, L. S. M. Alwis, F. Weigand, M. Kuhne, R. Heibig, and B. Roth, "Functionalized carbon reinforcement structures with optical fibre sensors for carbon concrete composites," in *Proc. Conf. Lasers Electro-Opt. Eur. Quantum Electron. Conf. (CLEO/Europe-EQEC)*, Jun. 2019, p. 1, doi: 10.1109/CI.FOF-EQEC.2019.8872285.
- [76] J. Hoffman, D. H. Waters, S. Khadka, and M. S. Kumosa, "Shape sensing of polymer core composite electrical transmission lines using FBG sensors," *IEEE Trans. Instrum. Meas.*, vol. 69, no. 1, pp. 249–257, Jan. 2020, doi: 10.1109/TIM.2019.2894045.
- [77] S. Mohanta, Y. Padarhi, J. Gupta, and S. Neogi, "Insight into the non-destructive performance evaluation of fiber-reinforced polymer composite laminate immersed in produced water using embedded fiber Bragg grating sensor," *Polym. Compos.*, vol. 42, no. 9, pp. 4717–4727, Jun. 2021, doi: 10.1002/pc.26181.
- [78] Z.-S. Guo, "Strain and temperature monitoring of asymmetric composite laminate using FBG hybrid sensors," *Struct. Health Monitor.*, vol. 6, no. 3, pp. 191–197, Sep. 2007, doi: 10.1177/14759217070060030201.
- [79] H.-K. Kang, C.-Y. Ryu, C.-S. Hong, and C.-G. Kim, "Simultaneous measurement of strain and temperature of structures using fiber optic sensor," *J. Intell. Mater. Syst. Struct.*, vol. 12, no. 4, pp. 277–281, Apr. 2001, doi: 10.1106/qwr3-fp25-ba1b-cx1x.
- [80] H.-K. Kang, D.-H. Kang, H.-J. Bang, C.-S. Hong, and C.-G. Kim, "Cure monitoring of composite laminates using fiber optic sensors," *Smart Mater. Struct.*, vol. 11, no. 2, pp. 279–287, Apr. 2002, doi: 10.1088/0964-1726/11/2/311.
- [81] H.-J. Yoon, D. M. Costantini, H. G. Limberger, R. P. Salathé, C.-G. Kim, and V. Michaud, "In situ strain and temperature monitoring of adaptive composite materials," *J. Intell. Mater. Syst. Struct.*, vol. 17, no. 12, pp. 1059–1067, Dec. 2006, doi: 10.1177/1045389X06064889.
- [82] S.-I. Takeda, T. Mizutani, T. Nishi, N. Uota, Y. Hirano, Y. Iwahori, Y. Nagao, and N. Takeda, "Monitoring of a CFRP-stiffened panel manufactured by VaRTM using fiber-optic sensors," *Adv. Compos. Mater.*, vol. 17, no. 2, pp. 125–137, Jan. 2008, doi: 10.1163/156855108X314760.
- [83] S. Minakuchi, "In situ characterization of direction-dependent cure-induced shrinkage in thermoset composite laminates with fiber-optic sensors embedded in through-thickness and in-plane directions," *J. Compos. Mater.*, vol. 49, no. 9, pp. 1021–1034, Apr. 2015, doi: 10.1177/0021998314528735.
- [84] T. Tsukada, S. Minakuchi, and N. Takeda, "Identification of process-induced residual stress/strain distribution in thick thermoplastic composites based on in situ strain monitoring using optical fiber sensors," *J. Compos. Mater.*, vol. 53, no. 24, pp. 3445–3458, Oct. 2019, doi: 10.1177/0021998319837199.
- [85] H. Hu, S. Li, J. Wang, L. Zu, D. Cao, and Y. Zhong, "Monitoring the gelation and effective chemical shrinkage of composite curing process with a novel FBG approach," *Compos. Struct.*, vol. 176, pp. 187–194, Sep. 2017, doi: 10.1016/j.compstruct.2017.04.051.
- [86] G. Zhang, Z. Zhou, G. Ding, S. Xu, C. Xie, and J. Zhang, "Cure monitoring and mechanical properties measurement of carbon fibre-reinforced plastics laminate using embedded fibre Bragg grating sensors," *Mater. Res. Innov.*, vol. 19, pp. S5-718–S5-725, May 2015, doi: 10.1179/1432891714Z.0000000001182.
- [87] Y. Qi, D. Jiang, S. Ju, and J. Zhang, "Investigation of strain history in fast and conventional curing epoxy matrix composites by FBGs," *Compos. Sci. Technol.*, vol. 159, pp. 18–24, May 2018, doi: 10.1016/j.compscitech.2018.02.019.
- [88] H. Rocha, C. Semprinoschnig, and J. P. Nunes, "Small-diameter optical fibre sensor embedment for ambient temperature cure monitoring and residual strain evaluation of CFRP composite laminates produced by vacuum-assisted resin infusion," *CEAS Space J.*, vol. 13, no. 3, pp. 353–367, Mar. 2021, doi: 10.1007/s12567-021-00357-5.
- [89] E. Oromichie, B. Gangadhara Prusty, P. Compston, and G. Rajan, "In-situ simultaneous measurement of strain and temperature in automated fiber placement (AFP) using optical fiber Bragg grating (FBG) sensors," *Adv. Manuf. Polym. Composites Sci.*, vol. 3, no. 2, pp. 52–61, May 2017, doi: 10.1080/20550340.2017.1317447.
- [90] V. P. Matveenko, N. A. Kosheleva, I. N. Shardaikov, and A. A. Voronkov, "Temperature and strain registration by fibre-optic strain sensor in the polymer composite materials manufacturing," *Int. J. Smart Nano Mater.*, vol. 9, no. 2, pp. 99–110, Mar. 2018, doi: 10.1080/19475411.2018.1450791.
- [91] V. P. Matveenko, I. N. Shardaikov, A. A. Voronkov, N. A. Kosheleva, D. S. Lobanov, G. S. Serovaev, E. M. Spaskova, and G. S. Shipunov, "Measurement of strains by optical fiber Bragg grating sensors embedded into polymer composite material," *Struct. Control Health Monit.*, vol. 25, no. 3, pp. 1–11, Mar. 2018, doi: 10.1002/stc.2118.
- [92] E. K. G. Boateng, P. Schubel, and R. Umer, "Thermal isolation of FBG optical fibre sensors for composite cure monitoring," *Sens. Actuators A. Phys.*, vol. 287, pp. 158–167, Mar. 2019, doi: 10.1016/j.sna.2019.01.001.

- [93] O. Frazão, R. Oliveira, and I. Dias, "A simple smart composite using fiber Bragg grating sensors for strain and temperature discrimination." *Microw. Opt. Technol. Lett.*, vol. 51, no. 1, pp. 235–239, Nov. 2008, doi: 10.1002/mop.23990.
- [94] M. Mulle, A. Yudhanto, G. Lubineau, R. Yaldiz, W. Schijve, and N. Verghese, "Internal strain assessment using FBGs in a thermoplastic composite subjected to quasi-static indentation and low-velocity impact." *Compos. Struct.*, vol. 215, pp. 305–316, May 2019, doi: 10.1016/j.compstruct.2019.02.085.
- [95] K. S. C. Kuang, R. Kenny, M. P. Whelan, W. J. Cantwell, and P. R. Chalker, "Embedded fibre Bragg grating sensors in advanced composite materials," *Compos. Sci. Technol.*, vol. 61, no. 10, pp. 1379–1387, Aug. 2001, doi: 10.1016/S0266-3538(01)00037-9.
- [96] T. Okabe and S. Yashiro, "Damage detection in holed composite laminates using an embedded FBG sensor." *Compos. A. Appl. Sci. Manuf.*, vol. 43, no. 3, pp. 388–397, Mar. 2012, doi: 10.1016/j.compositesa.2011.12.009.
- [97] S. Yashiro, N. Takeda, T. Okabe, and H. Sekine, "A new approach to predicting multiple damage states in composite laminates with embedded FBG sensors," *Compos. Sci. Technol.*, vol. 65, nos. 3–4, pp. 659–667, Mar. 2005, doi: 10.1016/j.compscitech.2004.09.022.
- [98] B. G. Prusty, "Failure investigation of top-hat composite stiffened panels." *Ships Offshore Struct.*, vol. 9, no. 2, pp. 186–198, Mar. 2013, doi: 10.1080/17445302.2012.759335.
- [99] J. L. F. Freire, V. A. Perrut, A. M. B. Braga, R. D. Vieira, A. S. Ribeiro, and M. A. P. Rosas, "Use of FBG strain gages on a pipeline specimen repaired with a CFRP composite." *Exp. Techn.*, vol. 39, no. 5, pp. 70–79, Sep. 2015, doi: 10.1111/j.1747-1567.2012.00866.x.
- [100] L. Yi, W. Zhenkai, and L. Jialu, "Research on health monitor for three-dimensional braided composite material." in *Proc. 3rd Int. Conf. Measuring Technol. Mechatronics Autom.*, Jan. 2011, pp. 1150–1153, doi: 10.1109/ICMTMA.2011.570.
- [101] P. Li and Z. Wan, "Study on the damages detection of 3 dimensional and 6 directional braided composites using FBG sensor," in *Proc. IEEE Symp. Ser. Comput. Intell. (SSCI)*, Dec. 2019, pp. 3272–3274, doi: 10.1109/SSCI44817.2019.9002784.
- [102] A. Rajabzadeh, R. Heusdens, R. C. Hendriks, and R. M. Groves, "Characterisation of transverse matrix cracks in composite materials using fibre Bragg grating sensors." *J. Lightw. Technol.*, vol. 37, no. 18, pp. 4720–4727, Sep. 15, 2019, doi: 10.1109/JLT.2019.2919339.
- [103] R. Fernández, N. Gutiérrez, H. Jiménez, F. Martín, L. Rubio, J. D. Jiménez-Vicaria, C. Paulotto, and F. Lasagni, "On the structural testing monitoring of CFRP cockpit and concrete/CFRP pillar by FBG sensors." *Adv. Eng. Mater.*, vol. 18, no. 7, pp. 1289–1298, Jul. 2016, doi: 10.1002/adem.201600065.
- [104] Y. J. Rao, S. F. Yuan, X. K. Zeng, D. K. Lian, Y. Zhu, Y. P. Wang, S. L. Huang, T. Y. Liu, G. F. Fernando, L. Zhang, and I. Bennion, "Simultaneous strain and temperature measurement of advanced 3-D braided composite materials using an improved EPPI/FBG system." *Opt. Lasers Eng.*, vol. 38, no. 6, pp. 557–566, Dec. 2002, doi: 10.1016/S0143-8166(02)00014-3.
- [105] K. Pran, O. Farsund, and G. Wang, "Fibre Bragg grating smart bolt monitoring creep in bolted GRP composite." *Proc. 15th Opt. Fiber Sensors Conf. Tech. Dig. (OFS)*, 2002, pp. 431–434, doi: 10.1109/OFS.2002.1000684.
- [106] D. Song, Z. Wei, J. Zou, S. Yang, E. Du, and H.-L. Cui, "Pressure sensor based on fiber Bragg grating and carbon fiber ribbon-wound composite cylindrical shell." *IEEE Sensors J.*, vol. 9, no. 7, pp. 828–831, Jul. 2009, doi: 10.1109/JSEN.2009.2024035.
- [107] C. S. Shin, B. L. Chen, J. R. Cheng, and S. K. Liaw, "Impact response of a wind turbine blade measured by distributed FBG sensors." *Mater. Manuf. Processes*, vol. 25, no. 4, pp. 268–271, Apr. 2010, doi: 10.1080/10426910903426448.
- [108] A. Panopoulou, D. Roulias, T. H. Loutas, and V. Kostopoulos, "Health monitoring of aerospace structures using fibre Bragg gratings combined with advanced signal processing and pattern recognition techniques." *Strain*, vol. 48, no. 3, pp. 267–277, Jun. 2012, doi: 10.1111/j.1475-1305.2011.00820.x.
- [109] P. Shrestha, Y. Park, H. Kwon, and C.-G. Kim, "Low velocity impact monitoring of composite wing structure under simulated wing loading condition using fiber Bragg grating sensors." in *Proc. 25th Opt. Fiber Sensors Conf. (OFS)*, Apr. 2017, Art. no. 103239B, doi: 10.1117/12.2267541.
- [110] L. Sun, J. Wang, H. Hu, C. Fu, C. Wang, and A. Ni, "A real-time NDT method based on FBG sensor spectrums to detect the transverse matrix cracks in composite materials." *J. Nondestruct. Eval.*, vol. 39, no. 2, pp. 1–12, Jun. 2020, doi: 10.1007/s10921-020-00687-0.
- [111] F. Falcatelli, A. Martini, A. Rivola, R. Di Sante, and M. Troncosi, "Strain modal testing with fiber Bragg grating sensors of composite components for automotive applications." in *Proc. IEEE Int. Workshop Metrol. Automat. (MetroAutomotive)*, Jul. 2021, pp. 181–186, doi: 10.1109/MetroAutomotive50197.2021.9502856.
- [112] Z. Wu, X. P. Qing, and F.-K. Chang, "Damage detection for composite laminate plates with a distributed hybrid PZT/FBG sensor network." *J. Intell. Mater. Syst. Struct.*, vol. 20, no. 9, pp. 1069–1077, Mar. 2009, doi: 10.1177/1045389X08101632.
- [113] B.-W. Jang, S.-O. Park, Y.-G. Lee, C.-G. Kim, and C.-Y. Park, "Detection of impact damage in composite structures using high speed FBG interrogator." *Adv. Compos. Mater.*, vol. 21, no. 1, pp. 29–44, Feb. 2012, doi: 10.1163/156855111X620874.
- [114] B.-W. Jang, Y.-G. Lee, J.-H. Kim, Y.-Y. Kim, and C.-G. Kim, "Real-time impact identification algorithm for composite structures using fiber Bragg grating sensors." *Struct. Control Health Monitor.*, vol. 19, no. 7, pp. 580–591, Apr. 2012, doi: 10.1002/stc.1492.
- [115] Y. Sai, M. Jiang, Q. Sui, S. Lu, and L. Jia, "FBG sensor array-based-low speed impact localization system on composite plate." *J. Mod. Opt.*, vol. 63, no. 5, pp. 462–467, Mar. 2016, doi: 10.1080/09500340.2015.1080864.
- [116] Y. Sai, X. Zhao, L. Wang, and D. Hou, "Impact localization of CFRP structure based on FBG sensor network." *Photon. Sensors*, vol. 10, no. 1, pp. 88–96, Mar. 2019, doi: 10.1007/s13320-019-0546-9.
- [117] Raju, A. Azmi, and B. Prusty, "Acoustic emission techniques for failure characterisation in composite top-hat stiffeners." *J. Reinforced Plastics Compos.*, vol. 31, no. 7, pp. 495–516, Feb. 2012, doi: 10.1177/0731684412437986.
- [118] Raju and B. G. Prusty, "Failure monitoring in composite structures using embedded FBG strain sensors." in *Proc. Photonics*, 2012, pp. 27–29, doi: 10.1364/photonics.2012.wpo.35.
- [119] S.-W. Kim, E.-H. Kim, M.-S. Jeong, and I. Lee, "Damage evaluation and strain monitoring for composite cylinders using tin-coated FBG sensors under low-velocity impacts." *Compos. B. Eng.*, vol. 74, pp. 13–22, Jun. 2015, doi: 10.1016/j.compositesb.2015.01.004.
- [120] T. Mizutani, N. Takeda, and H. Takeya, "On-board strain measurement of a cryogenic composite tank mounted on a reusable rocket using FBG sensors." *Struct. Health Monitor.*, vol. 5, no. 3, pp. 205–214, Sep. 2006, doi: 10.1177/1475921706058016.
- [121] Z. Wei, D. Song, Q. Zhao, and H.-L. Cui, "High pressure sensor based on fiber Bragg grating and carbon fiber laminated composite." *IEEE Sensors J.*, vol. 8, no. 10, pp. 1615–1619, Oct. 2008, doi: 10.1109/JSEN.2008.929070.
- [122] X. Geng, M. Jiang, L. Gao, Q. Wang, Y. Jia, Q. Sui, L. Jia, and D. Li, "Sensing characteristics of FBG sensor embedded in CFRP laminate." *Measurement*, vol. 98, pp. 199–204, Feb. 2017, doi: 10.1016/j.measurement.2016.12.003.
- [123] M. Ramakrishnan, G. Rajan, Y. Semenova, and G. Farrell, "Hybrid fiber optic sensor system for measuring the strain, temperature, and thermal strain of composite materials." *IEEE Sensors J.*, vol. 14, no. 8, pp. 2571–2578, Aug. 2014, doi: 10.1109/JSEN.2014.2306892.
- [124] G. Rajan, M. Ramakrishnan, Y. Semenova, G. Farrell, A. Domanski, A. Boczkowska, and T. Wolinski, "Performance analysis and comparison of composite materials embedded with different optical fiber sensor types." in *Proc. IEEE SENSORS*, Oct. 2011, pp. 351–354, doi: 10.1109/ICSENS.2011.6127055.
- [125] G. Rajan, M. Ramakrishnan, Y. Semenova, A. Domanski, A. Boczkowska, T. Wolinski, and G. Farrell, "Analysis of vibration measurements in a composite material using an embedded PM-PCF polarimetric sensor and an FBG sensor." *IEEE Sensors J.*, vol. 12, no. 5, pp. 1365–1371, May 2012, doi: 10.1109/JSEN.2011.2172412.
- [126] Y. Zhan, Z. Wang, A. Lu, F. Lin, Z. Song, and Z. Sun, "Optical fiber multiparameter sensor for real-time monitoring of thermoplastic composites during in situ consolidation process." *J. Appl. Polym. Sci.*, vol. 139, no. 1, pp. 1–10, Jan. 2022, doi: 10.1002/app.51450.

- [127] G. Luyckx, E. Voet, N. Lammens, W. De Waele, and J. Degrieck, "Residual strain-induced birefringent FBGs for multi-axial strain monitoring of CFRP composite laminates," *NDT & E Int.*, vol. 54, pp. 142–150, Mar. 2013, doi: [10.1016/j.ndteint.2012.11.008](https://doi.org/10.1016/j.ndteint.2012.11.008).
- [128] C. Sonnenfeld, S. Sulejmani, T. Geernaert, S. Eve, N. Lammens, G. Luyckx, E. Voet, J. Degrieck, W. Urbanczyk, P. Mergo, M. Becker, H. Bartelt, F. Berghmans, and H. Thienpont, "Microstructured optical fiber sensors embedded in a laminate composite for smart material applications," *Sensors*, vol. 11, no. 3, pp. 2566–2579, Feb. 2011, doi: [10.3390/s110302566](https://doi.org/10.3390/s110302566).
- [129] L. Q. Yu, A. I. Azmi, S. M. A. Musa, and R. K. R. Ibrahim, "Application of packaging technique in fiber Bragg grating temperature sensor for measuring localized and nonuniform temperature distribution," *Jurnal Teknologi*, vol. 64, no. 3, pp. 89–94, Sep. 2013, doi: [10.11113/jt.v64.2084](https://doi.org/10.11113/jt.v64.2084).
- [130] C. K. Y. Leung, Z. Yang, Y. Xu, P. Tong, and S. K. L. Lee, "Delamination detection in laminate composites with an embedded fiber optical interferometric sensor," *Sens. Actuators A, Phys.*, vol. 119, no. 2, pp. 336–344, Apr. 2005, doi: [10.1016/j.sna.2004.10.007](https://doi.org/10.1016/j.sna.2004.10.007).
- [131] E. Basile, A. Brotzu, F. Felli, C. Lupi, G. Saviano, C. Vendittozzi, and M. A. Caponero, "New magnetic connector for embedding of optical sensors in composite materials," in *Proc. 5th Int. Conf. Sens. Technol.*, Nov. 2011, pp. 521–526, doi: [10.1109/ICSENS.2011.6137034](https://doi.org/10.1109/ICSENS.2011.6137034).
- [132] H. Tsutsui, A. Kawamata, J. Kimoto, A. Isoe, Y. Hirose, T. Sanda, and N. Takeda, "Impact damage detection system using small-diameter optical-fiber sensors embedded in CFRP laminate structures," *Adv. Composite Mater.*, vol. 13, no. 1, pp. 43–55, Jan. 2004, doi: [10.1163/1568551041408813](https://doi.org/10.1163/1568551041408813).
- [133] G. Tsamasphyros, G. N. Kanderakis, C. Vrettos, and K. Kalkanis, "Numerical investigation of the optimum placement locations of optical fiber Bragg grating sensors for the health monitoring of bonded composite repairs," in *Proc. Macromolecular Symposia*, 2007, pp. 221–229, doi: [10.1002/masy.200750125](https://doi.org/10.1002/masy.200750125).
- [134] S. Khadka, J. Hoffman, and M. Kumosa, "FBG monitoring of curing in single fiber polymer composites," *Compos. Sci. Technol.*, vol. 198, pp. 1–8, Jun. 2020, doi: [10.1016/j.compscitech.2020.108308](https://doi.org/10.1016/j.compscitech.2020.108308).
- [135] S. Sharma, *Composite Materials: Mechanics, Manufacturing and Modeling*. Boca Raton, FL, USA: CRC Press, 2021.
- [136] W. D. Callister Jr. and D. G. Rethwisch, *Materials Science and Engineering—An Introduction*, 10th ed. Hoboken, NJ, USA: Wiley, 2018.
- [137] H. Song, W. Wang, Y. Zhou, and G. Zhou, "Mechanical properties of composites with embedded FBG sensors in different layer," in *Proc. IEEE 5th Int. Conf. Cybern. Intell. Syst. (CIS)*, Sep. 2011, pp. 52–56, doi: [10.1109/ICCIS.2011.6070301](https://doi.org/10.1109/ICCIS.2011.6070301).
- [138] K. Shivakumar and L. Emmanwori, "Mechanics of failure of composite laminates with an embedded fiber optic sensor," *J. Compos. Mater.*, vol. 38, no. 8, pp. 669–680, Apr. 2004, doi: [10.1177/0021998304042393](https://doi.org/10.1177/0021998304042393).
- [139] K. Shivakumar and A. Bhargava, "Failure mechanics of a composite laminate embedded with a fiber optic sensor," *J. Compos. Mater.*, vol. 39, no. 9, pp. 777–798, May 2005, doi: [10.1177/0021998305048156](https://doi.org/10.1177/0021998305048156).
- [140] T. O. Akinyemi, O. M. Omisore, G. Lu, and L. Wang, "Toward a fiber Bragg grating-based two-dimensional force sensor for robot-assisted cardiac interventions," *IEEE Sensors Lett.*, vol. 6, no. 1, pp. 1–4, Jan. 2022, doi: [10.1109/LSENS.2021.3133571](https://doi.org/10.1109/LSENS.2021.3133571).
- [141] V. Biazzi-Neto, C. A. F. Marques, A. Frizera-Neto, and A. G. Leal-Junior, "FBG-embedded robotic manipulator tool for structural integrity monitoring from critical strain-stress pair estimation," *IEEE Sensors J.*, vol. 22, no. 6, pp. 5695–5702, Mar. 2022, doi: [10.1109/JSEN.2022.3149459](https://doi.org/10.1109/JSEN.2022.3149459).
- [142] P. Zhu, P. Liu, Z. Wang, C. Peng, N. Zhang, and M. A. Soto, "Evaluating and minimizing induced microbending losses in optical fiber sensors embedded into glass-fiber composites," *J. Lightw. Technol.*, vol. 39, no. 22, pp. 7315–7325, Nov. 15, 2021, doi: [10.1109/JLT.2021.3112484](https://doi.org/10.1109/JLT.2021.3112484).
- [143] R. Franke, F. Hoffmann, and T. Bertram, "Observation of link deformations of a robotic manipulator with fiber Bragg grating sensors," in *Proc. IEEE/ASME Int. Conf. Adv. Intell. Mechatronics*, Jul. 2008, pp. 90–95, doi: [10.1109/AIM.2008.4601640](https://doi.org/10.1109/AIM.2008.4601640).
- [144] I. Payo, V. Feliu, and O. D. Cortázar, "Fibre Bragg grating (FBG) sensor system for highly flexible single-link robots," *Sens. Actuators A, Phys.*, vol. 150, no. 1, pp. 24–39, Mar. 2009, doi: [10.1016/j.sna.2008.11.033](https://doi.org/10.1016/j.sna.2008.11.033).
- [145] M. Kulpa, T. Howiacki, A. Wiater, T. Siwowski, and R. Sienko, "Strain and displacement measurement based on distributed fibre optic sensing (DFOS) system integrated with FRP composite sandwich panel," *Measurement*, vol. 175, pp. 1–14, Apr. 2021, doi: [10.1016/j.measurement.2021.109099](https://doi.org/10.1016/j.measurement.2021.109099).
- [146] H. J. Patrick, G. M. Williams, A. D. Kersey, J. R. Pedrazzani, and A. M. Vengsarkar, "Hybrid fiber Bragg grating/long period fiber grating sensor for strain/temperature discrimination," *IEEE Photon. Technol. Lett.*, vol. 8, no. 9, pp. 1223–1225, Sep. 1996, doi: [10.1109/68.531843](https://doi.org/10.1109/68.531843).
- [147] S. Zhang, X. Dong, T. Li, C. C. Chan, and P. P. Shum, "Simultaneous measurement of relative humidity and temperature with PCF-MZI cascaded by fiber Bragg grating," *Opt. Commun.*, vol. 303, pp. 42–45, Aug. 2013, doi: [10.1016/j.optcom.2013.04.008](https://doi.org/10.1016/j.optcom.2013.04.008).
- [148] X. Zhao, M. Dong, Y. Zhang, F. Luo, and L. Zhu, "Simultaneous measurement of strain, temperature and refractive index based on a fiber Bragg grating and an in-line interferometer," *Opt. Commun.*, vol. 435, pp. 61–67, Mar. 2019, doi: [10.1016/j.optcom.2018.11.022](https://doi.org/10.1016/j.optcom.2018.11.022).
- [149] X. Gui, Z. Li, X. Fu, H. Guo, Y. Wang, C. Wang, J. Wang, and D. Jiang, "Distributed optical fiber sensing and applications based on large-scale fiber Bragg grating array: Review," *J. Lightw. Technol.*, vol. 41, no. 13, pp. 4187–4200, Jul. 1, 2023, doi: [10.1109/JLT.2022.3233707](https://doi.org/10.1109/JLT.2022.3233707).
- [150] G. Souza and J. R. Tarpani, "Distributed fiber optics sensing applied to laminated composites: Embedding process, strain field monitoring with OBR and fracture mechanisms," *J. Nondestruct. Eval.*, vol. 39, no. 4, pp. 1–15, Oct. 2020, doi: [10.1007/s10921-020-00720-2](https://doi.org/10.1007/s10921-020-00720-2).
- [151] J. T. Tsai, J. S. Dustin, and J.-A. Mansson, "Distributed optical sensing for monitoring strain evolution during mechanical testing of composite laminates," *Polym. Test.*, vol. 96, pp. 1–9, Apr. 2021, doi: [10.1016/j.polymertesting.2021.107076](https://doi.org/10.1016/j.polymertesting.2021.107076).
- [152] M. Zhang, J. Wang, X. Xiong, Z. Chen, Y. Gong, S. Gao, and W. Zhang, "The strain distribution reconstructions using GWO algorithm and verification by FBG experimental data," *Appl. Sci.*, vol. 13, no. 3, p. 1-1259, Jan. 2023, doi: [10.3390/app13031259](https://doi.org/10.3390/app13031259).
- [153] M. Detka, "Reconstruction of strains with a non-smooth distribution using optical fiber Bragg grating," *Opt. Fiber Technol.*, vol. 62, pp. 1–7, Mar. 2021, doi: [10.1016/j.yofte.2021.102466](https://doi.org/10.1016/j.yofte.2021.102466).
- [154] G. Ding, F. Wang, X. Gao, and S. Jiang, "Research on deformation reconstruction based on structural curvature of CFRP propeller with fiber Bragg grating sensor network," *Photon. Sensors*, vol. 12, no. 4, pp. 1–13, Apr. 2022, doi: [10.1007/s13320-022-0656-7](https://doi.org/10.1007/s13320-022-0656-7).
- [155] I. Floris, J. M. Adam, P. A. Calderón, and S. Sales, "Fiber optic shape sensors: A comprehensive review," *Opt. Lasers Eng.*, vol. 139, pp. 1–17, Apr. 2021, doi: [10.1016/j.optlaseng.2020.106508](https://doi.org/10.1016/j.optlaseng.2020.106508).
- [156] F. Chen, X. Li, R. Wang, and X. Qiao, "Multiple cladding fiber Bragg gratings inscribed by femtosecond laser point-by-point technology," *J. Lightw. Technol.*, vol. 39, no. 23, pp. 7539–7544, Dec. 2021, doi: [10.1109/JLT.2021.3116206](https://doi.org/10.1109/JLT.2021.3116206).
- [157] Y.-G. Nan, I. Chapalo, K. Chah, X. Hu, and P. Megret, "Through overclad inscription of FBG in CYTOP optical fiber using phase mask technique and 400 nm femtosecond pulsed laser," *J. Lightw. Technol.*, vol. 40, no. 9, pp. 3031–3037, May 1, 2022, doi: [10.1109/JLT.2022.3144029](https://doi.org/10.1109/JLT.2022.3144029).
- [158] W. Gao, Y. Zheng, H. Bi, H. Guo, H. Yu, S. Jiang, and D. Jiang, "Drawing-tower inscription of apodized fiber Bragg grating arrays using a rotated focusing cylindrical lens," *Opt. Fiber Technol.*, vol. 68, pp. 1–7, Jan. 2022, doi: [10.1016/j.yofte.2021.102772](https://doi.org/10.1016/j.yofte.2021.102772).
- [159] P. Saccomandi, C. M. Oddo, L. Zollo, D. Formica, R. A. Romeo, C. Massaroni, M. A. Caponero, N. Vitiello, E. Guglielmelli, S. Silvestri, and E. Schena, "Feedforward neural network for force coding of an MRI-compatible tactile sensor array based on fiber Bragg grating," *J. Sens.*, vol. 2015, pp. 1–22, Aug. 2015, doi: [10.1155/2015/367194](https://doi.org/10.1155/2015/367194).
- [160] H. Choi, Y. Lim, and J. Kim, "Three-axis force sensor with fiber Bragg grating," in *Proc. 39th Annu. Int. Conf. IEEE Eng. Med. Biol. Soc. (EMBC)*, Jul. 2017, pp. 3940–3943, doi: [10.1109/EMBC.2017.8037718](https://doi.org/10.1109/EMBC.2017.8037718).
- [161] A. Datta, M. J. Augustin, N. Gupta, S. R. Viswamurthy, K. M. Gaddikeri, and R. Sundaram, "Impact localization and severity estimation on composite structure using fiber Bragg grating sensors by least square support vector regression," *IEEE Sensors J.*, vol. 19, no. 12, pp. 4463–4470, Jun. 2019, doi: [10.1109/JSEN.2019.2901453](https://doi.org/10.1109/JSEN.2019.2901453).



SITI MUSLIHA AISHAH MUSA received the B.Sc., M.Sc., and Ph.D. degrees in sciences (physics) from Universiti Teknologi Malaysia (UTM), in 2012, 2015, and 2021, respectively. She holds a postdoctoral position with Multimedia University. Before receiving her Ph.D. degree, she spent almost one year at Harbin Engineering University for her research attachment with full sponsorship from the Chinese Government Scholarship. She started her interest in fiber optics when she was an intern at Telekom Malaysia. She continued her passion by choosing fiber optic sensors as the topic for her final year project. Then, she began working on packed-bed non-thermal plasma reactor temperature profiling using fiber Bragg grating sensor for her master's degree project. With today's rapid technological advancements, she focuses her Ph.D. research on multiparameter sensing so that she can contribute to industry 4.0.



MOHD HAZIQ DZULKIFLI received the B.Eng. and Ph.D. degrees in mechanical engineering from Universiti Teknologi Malaysia, in 2013 and 2022, respectively. He is currently a Senior Lecturer with the Faculty of Mechanical Engineering, UTM. His current research interests include polymeric nanocomposite materials, focusing on matrix–reinforcement interfaces.



ASRUL IZAM AZMI received the B.Eng. and M.Eng. degrees in electrical engineering from Universiti Teknologi Malaysia (UTM), Skudai, in 2001 and 2004, respectively, and the Ph.D. degree from the University of New South Wales (UNSW), Sydney, in 2012. His Ph.D. was related to the area of optical fiber sensors and their applications in mechanical engineering. In 2002, he joined UTM as a Tutor and is currently an Associate Professor. He has been the Research Manager of the Faculty of Electrical Engineering with UTM, since 2022. His main research interests cover topics in optical sensors, including specialty fiber sensors, fiber lasers, fiber Bragg gratings, interferometric sensors, and spectroscopy-based sensors. His research focuses on the implementation of research findings into real-world applications.



SITI AZLIDA IBRAHIM (Senior Member, IEEE) received the B.Eng. degree (Hons.) in electronics majoring in telecommunications and the M.Eng.Sc. degree from Multimedia University (MMU), Malaysia, in 2002 and 2010, respectively, and the Ph.D. degree from Universiti Putra Malaysia (UPM), in 2017. She is a Researcher and an Academician working in the field of optical sensors. She has active research work in the area of optical fiber sensors, optical chemical sensors, gas sensors, micro/nano materials-based sensors, and dosimetry.

...